Graduate School ETD Form 9
(Revised 12/07)

PURDUE UNIVERSITY
GRADUATE SCHOOL
Thesis/Dissertation Acceptance

This is to certify that the thesis/dissertation prepared

By Nojan Aliahmad

Entitled
Paper-Based Lithium-Ion Batteries using Carbon Nanotube-Coated Wood Microfiber Current Collectors

For the degree of Master of Science in Electrical and Computer Engineering

Is approved by the final examining committee:

Kody Varahramyan
Chair

Mangilal Agarwal

Maher Rizkalla

Sudhir Shrestha

To the best of my knowledge and as understood by the student in the *Research Integrity and Copyright Disclaimer (Graduate School Form 20)*, this thesis/dissertation adheres to the provisions of Purdue University's "Policy on Integrity in Research" and the use of copyrighted material.

Approved by Major Professor(s): Kody Varahramyan

Approved by: Brian King 07/25/2013
Head of the Graduate Program Date

PAPER-BASED LITHIUM-ION BATTERIES USING CARBON NANOTUBE-COATED WOOD MICROFIBER CURRENT COLLECTORS

A Dissertation

Submitted to the Faculty

of

Purdue University

by

Nojan Aliahmad

In Partial Fulfillment of the

Requirements for the Degree

of

Master of Science in Electrical and Computer Engineering

August 2013

Purdue University

Indianapolis, Indiana

ACKNOWLEDGMENTS

I would like to express my appreciation to all who have supported and helped me throughout this research. I especially want to thank Professor Kody Varahramyan for providing this research opportunity, for his guidance through every step of my Master's Program, and for sharing his valuable knowledge with me. I gratefully thank Dr. Mangilal Agarwal and Dr. Sudhir Shrestha for their continuous support and advising throughout this research and the Master's Program. I would also like to thank Professor Maher Rizkalla for his advising and guidance in many aspects of my academic success.

I wish to express my thanks to Integrated Nanosystems Development Institute (INDI) for financial support, resources, and facilities. I would also like to thank Indiana University-Purdue University Indianapolis (IUPUI) for the opportunities and the support. Additionally, I would like to express my gratitude to my group members who helped me during this research, Mr. Ali Daneshkhah, Mr. Hossein Jafarian, Ms. Azadeh Hematti, Ms. Parvin Ghane, and Mr. Robbert Vittoe. I would also like to thank Dr. Yadong Liu, Dr. Jian Xie, and Dr. Youngsik Kim for laboratory assistance, as well as the School of Engineering and Technology, and Department of Electrical and Computer Engineering for the opportunities and support; and Dr. Brian King, Ms. Valerie Lim Diemer, and Ms. Sherrie Tucker for their support and guidance.

TABLE OF CONTENTS

Page

LIST OF TABLES

LIST OF FIGURES

Figure Page

ABSTRACT

Aliahmad, Nojan. MSECE, Purdue University, August 2013. Paper-Based Lithium-Ion Batteries using Carbon Nanotube-Coated Wood Microfiber Current Collectors. Major Professor: Kody Varahramyan.

The prevalent applications of energy storage devices have incited wide-spread efforts on production of thin, flexible, and light-weight lithium-ion batteries. In this work, lithium-ion batteries using novel flexible paper-based current collectors have been developed. The paper-based current collectors were fabricated from carbon nanotube (CNT)-coated wood microfibers (CNT-microfiber paper). This thesis presents the fabrication of the CNT-microfiber paper using wood microfibers, coating electrode materials, design and assemblies of battery, testing methodologies, and experimental results and analyses.

Wood microfibers were coated with carbon nanotubes and poly(3,4-ethylenedioxythiophene) ($PEDOT$) through an electrostatic layer-by-layer nanoassembely process and formed into a sheet, CNT-microfiber paper. The CNT loading of the fabricated paper was measured 10.1 $\mu g/cm^2$ subsequently considered.

Electrode material solutions were spray-coated on the CNT-microfiber paper to produce electrodes for the half and full-cell devices. The CNT current collector consists of a network structure of cellulose microfibers at the micro-scale, with micropores filled with the applied conductive electrode materials reducing the overall internal resistance for the cell. A bending test revealed that the paper-based electrodes, compared to metal ones, incurred fewer damages after 20 bends at an angle of 300°. The surface fractures on the paper-based electrodes were shallow and contained than

metallic-based electrodes. The micro-pores in CNT-microfiber paper structure provides better adherence to the active material layer to the substrate and inhibits detachment while bending.

Half-cells and full-cells using lithium cobalt oxide (LCO), lithium titanium oxide (LTO), and lithium manganesium oxide (LMO) were fabricated and tested. Coin cell assembly and liquid electrolyte was used. The capacities of half-cells were measured 150 mAh/g with LCO, 158 mAh/g with LTO, and 130 mAh/g with LMO. The capacity of the LTO/LCO full-cell also was measured 126 mAh/g at $C/5$ rate. The columbic efficiency of the LTO/LCO full-cell was measured 84% for the first charging cycle that increased to 96% after second cycle. The self-discharge test of the full-cell after charging to 2.7 V at $C/5$ current rate is showed a stable 2 V after 90 hours.

The capacities of the developed batteries at lower currents are comparable to the metallic electrode-based devices, however, the capacities were observed to drop at higher currents. This makes the developed paper-based batteries more suitable for low current applications, such as, $RFID$ tags, flexible electronics, bioassays, and displays. The capacities of the batteries at higher current can be improved by enhancing the conductivity of the fibers, which is identified as the future work. Furthermore, fabrication of an all solid state battery using solid electrolyte is also identified as the future work of this project.

1. INTRODUCTION

1.1 Lithium-ion batteries

Lithium-ion batteries are widely used due to their high energy densities compared to their sizes. Having a smaller energy storage device with higher capacity is the main goal of lithium-ion batteries. These cells are much lighter than more conventional batteries such as alkaline, lead acid, and nickel cadmium cells while they can provide better capacities [1]. Figure 1.1 shows the relationship between the specific power and specific energy of different types of batteries in different current rates. As it is shown, lithium-ion batteries can provide the highest specific power and specific density in all current rates compared to the other types of batteries.

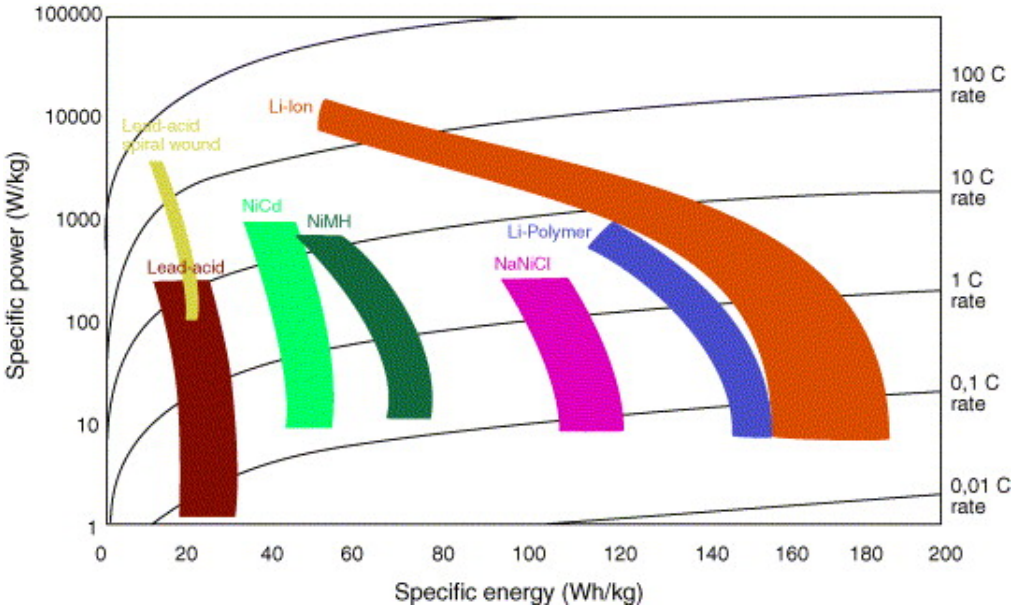

Fig. 1.1. Specific and specific power of different batteries [2]

Table 1.1
Performance comparison of different types batteries [4]

	Lead acid	NiMH	NiNaCl	Lithium-ion
Nominal cell voltage (V)	2	1.2	2.58	2.5/3.3/3.6-3.7
Specific energy (Wh/kg)	30-45	30-80	90-100	90-220
Energy density (Wh/L)	60-75	140-300	160	280-400
Specific power (W/kg)	180	250-1000	150	600-3400
Cycle life	500-800	500-1000	1000	1000-8000
Self-discharge (%/month)	2-4	20-30	0	2-5
Temperature range (°C)	-20-60	-20-60	270-350	20-60
Costs	Low	Moderate	low	High

Lithium-ion batteries also provide longer cycle life compared to other types of batteries. The numbers of working cycles of lithium-ion cells are 10 times higher than other kinds of batteries. Furthermore, the voltage range of these devices is higher. They can provide a wide range of voltage from 2.5 V to nearly 4 V [3]. Table 1.1 shows a comparison between different types of batteries. The table shows that the energy density, specific energy, and specific power of lithium-ion batteries are about two times higher than lead acid and nickel based batteries, however the fabrication costs of lithium-ion batteries are higher. It can also be observed that lithium-ion cells could provide longer cycle life with lower self-discharge rate.

The vast effort of research and development in fabrication of reliable, safe, and durable energy storage devices resulted in the creation of lithium-ion batteries. While the first non-rechargeable lithium-ion battery was developed in 1970s using lithium metal anode and a TiS_2 cathode with an organic liquid electrolyte, the first rechargeable lithium-ion battery was fabricated using lithium metal anode and graphite cathode in the 1980s [3, 5]. This cell could produce high voltage and capacity; however

it failed because of safety issues and explosive reactions of its lithium metal anode. Using non-metallic lithium salts in electrodes of lithium-ion batteries over metallic current collectors was a solution to overcome the safety problems of the first generation of the lithium-ion batteries. Finally the first commercial lithium-ion battery was produced by Professor John Goodenough in 1991. These batteries used lithium, cobalt, manganese, and nickel compounds in their anodes instead of the lithium metal. Further research showed to produce the different output voltages, different anode and cathode lithium salts could be used [1, 3, 6].

Although during the last two decades most of the lithium-ion battery researches were focused on developing new lithium compounds [7]. Form early years of 21st century other aspects of the lithium ion batteries such as current collectors [8, 9], separators, and electrolytes [1] also became subject of research. One of the areas for research was the electron collector. Replacing this part with non-metallic components and providing some features such as better flexibility and longer life were two goals of such research.

For more than two decades, the research has been conducted to fabricate safer lithium-ion batteries, while providing higher capacity. Fabrication of the layered crystals is a solution to achieve higher capacity with longer life. Iron, nickel, vanadium, and aluminum particles are inserted into the lithium compounds to provide better conductivity [7]. Layered materials can provide better cycle life due to less ion trapping, solid electrolyte interface formation and easier ion transportation inside the electrodes. A research shows that spinel structures can also increase the performance of the active materials. Lithium manganese oxide is one of the materials that can be found in both regular and spinel forms. The spinel crystals (isometric) are working longer while they are environmental friendly [10, 11]. Furthermore lithium, cobalt, nickel and copper alloys also can provide high performance crystals [12].

Beside the electrode materials, other parts of the battery play a role in the overall performance of them. Optimization of the lithium-ion cell can be made through current collectors, electrolyte or separators. Using nano materials inside the electrodes can provide better stability for cell. Using silicon and titanium electrodes can provide more flexibility and mechanical stability [1]. Porous metals oxides can also be another solution for flexible lithium-ion batteries. These metals can provide better flexibility and stability for lithium-ion cells [13]. In addition, novel materials are used for current collector fabrication such as carbon nanotube or other conductive polymers. Research shows that these materials can provide higher conductivity and better performance [14–16]. Separators have also been improved during the last decade. The most important part that can affect the internal resistance of a battery is its separator. The ionic conductivity of the separators are between 10^{-5} to 10^{-3} S/cm but there are more researches to improve this value and combine them with electrolyte to provide all solid state battery. Different polymers and ceramics are fabricated and tested to work as the separator and solid electrolyte. These materials can increase the performance of the cell, while they can increase the safety of the lithium-ion batteries [17–21].

In any lithium-ion battery a medium is used to transfer ions is called an electrolyte. Electrolytes are mainly separated by their states. The electrolyte can be solid or liquid. In an all solid state battery the liquid electrolyte and polymer separator are mixed together and form a solid or gel ionic conductive medium between the anode, and the cathode called solid electrolyte. Using a polymer layer mixed with an ionic conductive salt, the first solid state electrolytes were prepared [3].

Having high specific energy and energy density are the most important advantages of lithium-ion batteries. Moreover, lower self-discharge rate, higher cycle life, and faster charging and discharging time make these batteries suitable for many applications. Although the lithium-ion batteries have many advantages in comparison

with other types of batteries, safety issues, electrode degradation, flexibility, weight, and production costs are some of the drawbacks of these devices [3, 22–24].

1.2 Flexible lithium-ion batteries

The increasing demand of lithium ion batteries for new applications has provided an impetus to the efforts to produce more flexible batteries. Future electronic devices, most importantly low power wide application devices such as $RFID$ tags, implantable medical devices, sensors, and flexible displays will need flexible source of energy [25]. Growing the technology of polymers and nano materials could provide enough foundation to fabricate an all solid state flexible battery.

The first step to creating a flexible lithium ion battery is the fabrication of thin film lithium ion batteries. Thin film batteries are similar to the regular lithium ion batteries while the thickness of these devices is limited between hundred nano to a few micrometers. In these devices, all parts such as electrolyte, separator, substrate, anode, and cathode must be developed in nano or micro scale. The cathode and anode materials of these cells are regular lithium salts made by metal oxides [18]. The electron collector of these devices must be very thin and should have a high surface area. Nano conductive materials are the best solution to provide the electron collector surface for these cells. The electrolyte is the most important part in these cells, which is quite different than regular lithium ion batteries. The electrolyte of these devices must meet the safety standards while providing reasonable flexibility with thickness of a few tens of micrometers. $LiPON$ is one of the polymers widely used in thin film batteries. This material is a solid-gel electrolyte, so the thin film batteries are usually made in all solid state form [20, 26].

Another gel electrolyte for thin film batteries is made using polyacrylonitrile (PAN) as the main structure for the solid electrolyte. The process starts by mixing the PAN with lithium hexafluorophosphate ($LiPF_6$), ethylene carbonate (EC), Dimethyl ether (DME) with (10%,4%,60%,20% molar ratio). Then Al_2O_3 is added to the solution to develop the solid electrolyte. This polymer needs a heat treatment for 30 seconds with the temperature of 90°C to form a gel film with a thickness of $100\mu m$ [17, 27]. Polyethylene oxide (PEO) and poly acrylic acid (PAA) are other polymers that can also be used to fabricate a thin ionic conductive layer. PEO/PAA is a strong lithium-ion conductive in the range of 10-5 to 10-4 S/cm and can be used in thin film batteries, Poly(methacrylic acid) ($PMAA$) can also be used instead of PAA with PEO [15, 28, 29].

The current collector is another part of a lithium-ion battery that can be improved to provide more flexibility and better performance. To create a very high surface area and conductivity for current collectors, different materials are produced. Silicon nanowires and carbon nanotubes are some of these materials [30, 31]. One of the impacts in flexible batteries technology has been presented by development of CNT. Flexible batteries that are made over CNT sheets can be stronger than metallic cells. The CNT-coated conductive sheets (buckypapers) and the thin films of CNT over a substrate are suitable alternatives for the metallic current collectors. These current collectors can deliver higher electron mobility while providing a flexible substrate for active materials. Although these materials are very advantageous, they increase the fabrication costs of the lithium-ion battery due to the huge amount of CNT utilization [9, 25, 31]. Likewise nonmetallic substrates have also been fabricated using silicon [30] or zinc oxide layer over carbon fiber sheets [8]. All of these presented methods use nanoscale properties to provide a flexible, thin, and better conductive current collector for lithium-ion batteries.

Researchers have shown that the current collectors made by CNT ink can be used inside the lithium ion batteries. The CNT ink was prepared from CNT materials and other conductive nanoparticles such as silver (Ag) nanowires. These highly conductive materials are mixed with ethylene glycol (EG) and polyvinylprrolidone (PVP) [9, 31]. The fabricated ink is highly conductive while it could disperse better in a solvent due to the usage of polymer binders. Better dispersion of the materials inside the solvent can provide more uniform conductive films. This ink then is deposited over a PET, or paper substrate to provide conductive surfaces. The thickness of this layer over the paper is measured about 100nm to 5m and it could be twisted down to a 2-mm radius [9]. This paper is robust in contact with acids and lithium-ion electrolyte solvents. The amount of CNT utilization to produce the conductive paper is measured between 1.33 to 1.7 mg/cm^2. The lithium titanium oxide and lithium manganese oxide half-cells made by this paper as the current collector show the capacity of 149 mAh/g and 110 mAh/g for c/3 rate which are comparable with metallic based devices. Further studies showed that current collectors made by CNT ink can also be used in full-cell configuration and produce a good performance. A lithium titanium oxide/lithium cobalt oxide full-cell which is made by the CNT ink based current collector could also produce comparable results with regular cells [31].

CNT is widely used in other energy storage devices such as super capacitors. The huge surface area of the CNT rods makes them one of the best candidates for energy storage devices. CNT based capacitors can provide higher cycle life, better capacitance and lower production costs. Due to the characteristics of CNT these devices can provide higher specific power and specific energy at the same time. These abilities make them a perfect material for high power capacitors [14,32]. Double layer super capacitors ($EDLC$) can be made by single wall carbon nanotubes ($SWNT$). The carbon nanotube film sandwiched between the layers of Pt sheets that form the current collectors of the capacitor and make an $EDLC$. These capacitors can operate up to 2.5 V with the capacitance of 20 F/g. The energy density of these devices was

also measured at 69.4 Wh/kg [33, 34]. The maximum power density of these CNT based capacitors can reach up to 43.3 kW/kg and 24 kW/kg for thicknesses of 100 and 500 μm, respectively. Moreover, the $EDLC$ devices can reach the energy density of 0.5 to 10 Wh/kg and they could provide a huge working cycle. One of the drawbacks of these devices compared with the batteries is their discharging time. CNT based $EDLC$ devices cannot store energy for a long time compared to other energy storage devices. Their useful time of operation is less than 0.01 seconds in comparison with lithium-ion batteries which are used for cycles longer than 100 seconds [34].

CNT can be made by different methods. High-pressured Carbon Monoxide ($HiPco$) CNT is one of the commercially available CNT that can be used for different energy applications. $HiPco$ process for CNT rod fabrication is used because of its wide range of concentration and flexibility. These CNT rods have a diameter of 0.8 to 1.2 nm and the length of 100 nm to 1 μm. The dimension of these CNT rods is the reason for having a high surface area. The conductivity of these rods theoretically is 1000 times greater than copper [35]. Recent research shows that the sheet resistance of a CNT ink over a standard paper has the sheet resistance of 30 Ω/sq and the bucky paper made by a $HiPco$-CNT has a sheet resistance resistant of 0.2 to 2 Ω/sq [9]. Furthermore, the CNT ink over the paper is more persistence for bending in comparison with gold coated paper [9, 31]. CNT rods are also widely used in LbL nano assemblies. CNT rods with a polymer like poly(sodium 4-styrene-sulfonate) (PSS) can be deposited over different substrates, such as paper, ITO glass, and polymer substrates such as PET films [14, 31, 36]. These capabilities of the CNT, makes it a suitable material for the LbL process and in forming conductive surfaces using nanofabrication techniques.

Lithium-ion batteries made with flexible substrates utilize different types of active materials, including $LiMn_2O_4$, $LiCoO_2$, and $Li_4Ti_5O_{12}$ [9, 31]. The voltage of these materials range between 0.8 to 4.3 V and it has been shown that the CNT does not

react in contact with these active materials. Regular active materials, and the liquid electrolyte are also used in CNT-based cells [37].

Another impact in the fabrication of flexible cells is started by the development of polymer technology. Ionic conductive polymers like polyethylene oxide (PEO) and polyvinylidene fluoride ($PVDF$) were introduced to the market in the 1980s. Although these materials have been used in many applications, since the beginning of the 21st century many researches have been conducted to find a solution about using these polymers in a solid state lithium-ion battery as the solid electrolyte. Although the ionic conductivity of these films is about 10 to 100 times lower than the liquid electrolytes which are in the range of 10^{-4} to 10^{-5} S/cm, the importance of having all solid state cells make them attractive for research [28, 38].

1.3 Research Objectives

The purpose of this research is to produce a thin, flexible and light-weight lithium-ion battery using paper-based materials. The batteries introduced in this thesis use flexible paper-based current collectors (CNT-microfiber paper) which are specifically developed for this purpose. These current collectors are fabricated by forming a sheet of conductive paper using CNT-coated wood microfibers through a layer-by-layer (LbL) nanoassembly process. The conductivity and the battery results of the paper is comparable with metallic current collectors while it is more flexible and provides a better surface contact with the active material. The CNT-microfiber paper must work with different kinds of active materials in different working voltages and must meet the safety standards such as low working temperatures and non-explosive chemical reactions. The conductivity of the paper with the thickness of 50 μm is measured 1.94 $k\Omega$-cm. The conductivity of the paper results in providing a low resistance paper.

While CNT is widely used to produce high quality conductive materials, fabrication of a CNT-microfiber paper can be a solution to produce flexible lithium-ion batteries. High conductivity and flexibility of the fibers can be used to overcome some of the problems of lithium-ion batteries such as high capacity, better flexibility, and lower weight. Achieving commercially competitive CNT-based current collectors will require further reduction in CNT utilization. Devices presented in this research are made by the LbL technique to allow the construction of composite multilayered coating at nanoscale, which brings novel properties to the substrate (wood microfibers) through the alternate deposition of oppositely charged polyelectrolytes and/or nanoparticles [14, 39]. Using LbL process can preserve its texture and porous structure. The amount of CNT utilization also reduces to only 0.2% by wt., which represents a significant reduction. Furthermore, the LbL process can produce a uniform and quite precise conductivity for the paper-based current collectors.

The fabrication and usage of CNT-microfiber paper as current collectors in lithium-ion batteries represents the novel aspect of this research. Fabricated CNT-microfiber paper is tested through both half-cell and full-cell configuration to check the stability of the paper in contact with different materials with wide range of voltages up to 4.3 V. Other tests, such as a long time test with different current rates are also provided to find the optimum working conditions of the cells. Finally the electrodes are examined through a bending test to compare the flexibility with metallic ones. SEM imaging is also conducted to study the surface structure, thickness of the paper and the active material layer, connections between the active material with the paper fibers, and the structure of electrodes. The paper based current collector is observed to meet all the requirements of a metallic current collector through this investigation. The steps from the formation of CNT-microfiber paper current collectors, assembly of the batteries and the experimental results of the experiments are presented.

2. THEORY

2.1 Lithium-ion batteries

Lithium is one of the smallest metallic atom with the atomic weight of 6.94, standard potential of -3.05 V and electrochemical weight of 3.86 Ah/g [3]. The high standard electrode potential and light weight of this element make it a proper choice for electrodes for high energy density energy storage devices. Lithium and its compound metallic salts are widely used in energy storage devices due to their characteristics such as high specific energy and high energy density. These devices can provide a low self-discharge rate while having a long cycle life. The combination of these benefits, in addition to other benefits such as size, weight, and safety, make these devices a suitable solution for energy storage applications in portable electronic devices, communication devices, and hybrid cars. In these batteries, due to the migration of the lithium ions between electrodes using an electrolyte, lithium cannot stay in its metallic state, either in the charge or the discharge process. So these batteries are called lithium-ion batteries [3, 40].

Lithium-ion batteries consume lithium storage materials as the active materials of both electrodes. During a cycle, lithium ions travel between the negative and the positive electrodes repeatedly. In each charging and discharging cycle, lithium ions are extracted or inserted to the transitional layers inside the active materials. The characteristics of a battery, such as capacity or specific voltage, are defined by the active materials of each electrode. Positive electrodes are mostly made by metal oxides such as lithium cobalt oxide ($LiCoO_2$), lithium manganese oxide ($LiMn_2O_4$), lithium iron phosphate ($LiFePO_4$), lithium nickel manganese cobalt oxide ($Li(NiMnCo)O_2$), lithium nickel magnesium aluminum oxide ($Li(NiCoAl)O_2$) over an aluminum cur-

rent collector. Negative electrodes are made by graphite carbon or another metal oxide material such as $Li_4Ti_5O_{12}$ over a copper current collector. Other materials such as Si nanowires or nano material compounds made by Sn-Co-C alloys are also introduced as active compounds for lithium-ion batteries. Matching these materials in negative and positive materials can provide different advantages such as stability, cycle life, production costs, and other capabilities for specific application [3, 19, 41].

During the charging cycle, electrons are released from the cathode. This causes the oxidation of the lithium salt and the loss of lithium ions. These free ions pass through the separator and migrate from the cathode to the anode using the electrolyte medium. In the anode lithium ions react with the free electron and complete the circuit. On the other hand, in the discharging cycle the lithium ions leave the anode and come back to the cathode [42]. Figure 2.1 shows the migration of lithium ions in both half-cell and full-cell configuration.

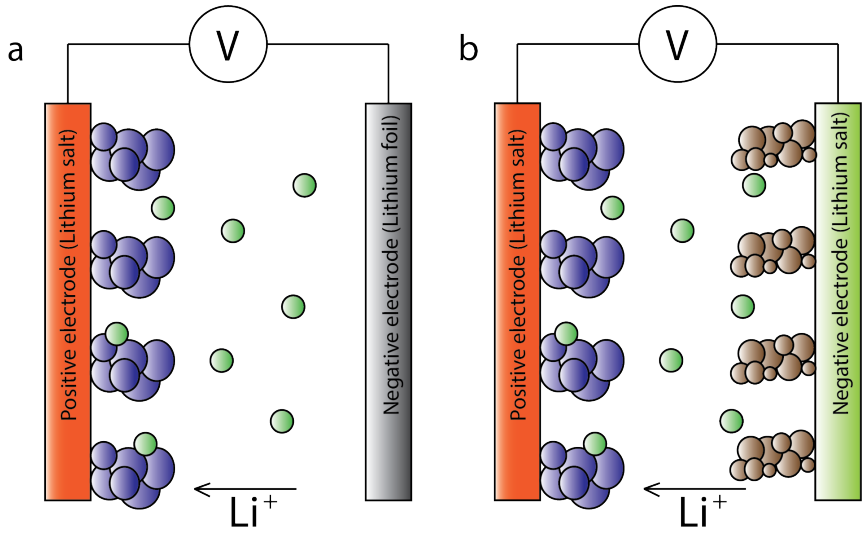

Fig. 2.1. Schematic of (a) half-cell and (b) full cell operation

Each charge and discharge process is called a cycle. Lithium-ion batteries can provide cycles from few hundred to thousands of cycles in their working life [43]. A

perfect voltage range without making overcharges is one of the important factors that can increase the cycle life of a cell. In addition, lithium-ion batteries are temperature sensitive. The working temperature of these devices is between -40 to 80°C, although the best working range of these cells to provide better working life is between 20 to 40°C. In higher temperatures reactions inside the cell between the electrolyte and cathode will happen and cause the degradation of the materials. Furthermore, in higher temperatures thermal runway effect can happen. This means that the electrons can jump through the separator from the anode to the cathode or vice versa and provide short circuits inside the cell [44]. Finally, higher temperatures can increase the chemical reactions inside the cells that can produce gases which lead to the destruction of the cell [3].

In detail, during each charging cycle, lithium ion is deduced from the cathode active material because the electrons of the active material are released from the cathode through the external circuit. These free lithium ions travel to the anode and after lithium is migrated to the interlayers of the active materials in the anodes it reacts with an extra electron inserted into the anode and becomes stable. Equally, during each discharge cycle lithium is deduced from interlayers of the anodes, and migrates back to the cathode. The reversible incorporation of lithium in an intercalation reaction causes the lithium ions to move from or to be imported into the structure of active material using tunneling or forming a layer over that. This process is related to the structure of the material, so for lithium salts, tunneling can happen, while for graphite the oxide layer formation is occurs [19, 44].

The equations 2.1 can show the oxidation and reduction process inside the cell [3]:

$$\begin{aligned} &\text{LiA} \rightarrow A + Li^{n+} + ne^{-} \text{ (oxidation)} \\ &\text{B+Li}^{n+} + ne^{-} \rightarrow LiB \text{(reduction)} \\ &\text{LiA} \leftrightarrow A + Li^{n+} + ne^{-} + B \leftrightarrow LiB \text{ (redox reaction)} \end{aligned} \tag{2.1}$$

The capacity of a lithium-ion battery is related to the active material, the internal impedance of the cell, the operation condition, and the C rate of the battery. The theoretical capacity of a cell is related to the type of active material only, and it is a capacity that fully charged batteries can release in each discharging cycle, ideally. There is a small resistance inside the cell due to the impedance of the parts, formation of solid-electrolyte interphase (SEI) and other slow electrochemical processes a small of the charge cannot be delivered from the cell. These phenomena can be seen by a voltage drop after starting to discharge a cell [45]. Figure 2.2 shows the range of capacity of different materials. Although Lithium metal can provide the highest capacity, it is not safe to be used inside the commercial batteries. There are some novel materials based on nitrides, silicon, and graphite that can produce better capacities than lithium salts but this working voltage is problematic. On the other hand, lithium salts can provide higher voltage up to 4.3 V but their problem is lower capacity. Today there is much research being conducted to find other materials that can provide higher capacities with higher working voltages.

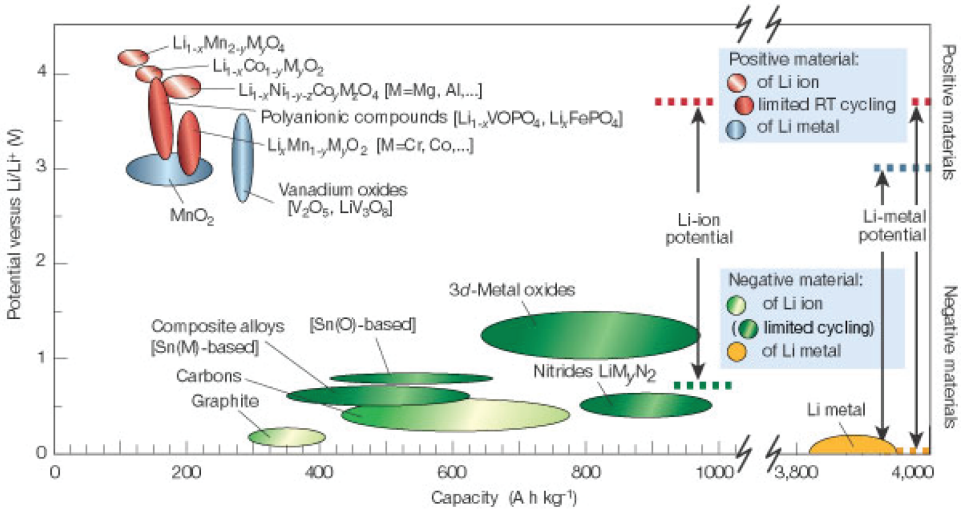

Fig. 2.2. Voltage vs. capacity for positive and negative electrode materials [1]

During the cycle life of a lithium-ion battery, some physical and chemical reactions cause the capacity degradation inside the cell. The capacity drop during cycles and rest time of a cell can happen due to these degradations [46]. The capacity of a cell is defined by the equation 2.2 where Q is the capacity, t is the time of discharge/charge and I is the discharge/charge current [3]:

$$Q = \int_{0-t} I dt \tag{2.2}$$

Another term related to the capacity is the rated capacity. This parameter is used to show the capacity fade of the battery. C rate shows the amount of capacity that a cell can deliver. The equation 2.3 shows the rate capacity [3].

$$C_{rate} = I/Q \tag{2.3}$$

This means that if a battery charged over a 1 hour period of time, it was charged in $1C$ rate. Meanwhile, if it is discharged or charged again in 2 hours the C rate will be $1/2C$ [46]. C rates are not accurate for all cells. Although the C rate should be related to the material of the cell, sometimes all the charge stored inside a cell cannot be used by the outside source and the internal resistance of the cells can change this number.

The degradation of a lithium-ion battery can be divided in two sections. The first type of degradation is normal degradation. This degradation occurs due to the cycling of the cell. This drop is high in first few charge/discharge cycles of the battery. After that the speed of this degradation become slower and the battery stays in a stable state of charge. In the end of the cycle life (last few cycles) of the battery again this degradation becomes faster and more rapid [47]. The normal capacity degradation of the cell is related to many reactions inside the cell. First of all SEI formation is the main reason of that. In first few cycles the SEI layer forms over the anode and

traps some of the cyclable lithium ions of the cell. After first few cycle by reducing the speed of SEI formation, the capacity fade becomes limited. Another important factor of normal degradation of a lithium-ion battery is the degradation of the active materials. This type of degradation which is more affective after couple of cycles is massive in cathode electrode. In this case the lithium salts start to react with the lithium ions and trap the cyclabe lithium ions. This process can also limit the capacity of the battery [19, 45].

Some other degradation can also happen due to the operation conditions of the lithium-ion battery such as temperature, charging currents, and depth of charge. Working temperature is very important for lithium-ion batteries. In most of cases this temperature must be between 20 to 40°C. Higher temperatures can increase the chemical reactions inside the cell and decompose the lithium salts. Lower temperatures also can reduce the speed of chemical reactions and prevent the ion transfer process inside the cell. Using high current can also limit the life of the battery. In each cycles lithium ions travel from one electrode to another one. This means that a huge amount of ions fill out the surface of the electrode. Increasing the current will increase the amount of these ions over the electrode. This pile of ions need time to react with the active material. By increasing the current the internal resistance of the cell becomes higher due to this phenomenon. Keeping a huge amount of ions over the electrodes can also destroy the active material layer. High currents push the ions to react with the surface layers of active materials and this can prevent the penetration of free ions to the internal layers and reduce the capacity of the battery [45, 47]. Finally overcharging the cell can also damage the capacity and cycle life of that. Each active material has a stress point which is related to its structure. In overcharging, more ions are pushed into the electrode while there is no free space for them. This can increase the resistance of the cell by providing a layer of ions over the electrode. In addition higher voltages can lead up to the oxidation of the active material, decomposition of the binder and destroying the structure of the electrolyte lithium salts.

Over discharging can also provide capacity drop of lithium-ion batteries. In over discharging process the current collectors can be dissolved into the electrolyte. This can increase the impedance of the cell and reduce the capacity. In addition, higher voltages can increase the chance of active material migration. In higher voltages, instead on lithium ions, the whole crystal of lithium slat will migrate from anode to cathode and pinch through the separator. This can destroy the separator and cause short circuits inside the cell, while providing capacity fading [45].

2.1.1 Electrode materials

Lithium salts are widely used inside the electrodes of lithium-ion batteries widely as the active materials. These lithium salts form a safe and reliable electrodes for lithium-ion batteries and can be used both in the anode and the cathode regarding their voltage range. The anode is the negative electrode and the cathode is the positive electrode of a lithium-ion battery. During the charging time, the ions migrate to anode and in discharge the ions leave the anode and travel back to the cathode. In metallic cells, the anode current collector is usually made by a copper foil and the cathode current collector is usually made by aluminum [9]. Here are some of the active materials which are consumed in this research with their specifications and fabrication processes.

$LiMn_2O_4$

There are different methods to produce this material such as solid state reaction, solution synthesis, and the freezing-drying method. Among all of these methods, solution synthesis is one of the simplest. In this method, $CH_3COOLi2H_2O$, and $Mn(CH_3COO)_24H_2O$ are mixed and ground with adipic acid with the molar ratio of 1:2:3. The final mixture of these three powders is dissolved in the deionized water,

and heated up to 80°C for about 10 hours. In the next step, the gel is formed by this process is distillated and the final product is heated up to 400°C for another 8 hours. The final product of this step is ground and received another heat treatment with the temperature of 600-800°C for 10-30 hours [10].

This material has a cubic crystal structure and its maximum capacity can be reached about 100-148 mAh/g, a suitable material for anodes of lithium-ion batteries. The voltage range of this crystal is also between 2.8 to 4 V [11]. Figure 2.3 shows the crystal structure of this particle.

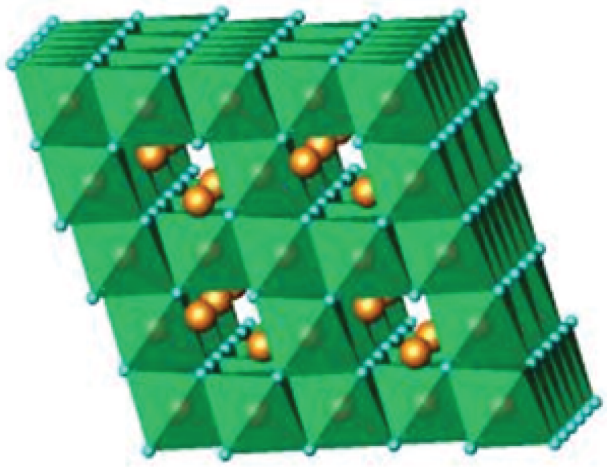

Fig. 2.3. Crystal structure of $LiMn_2O_4$ [48]

The chemical reaction of $LiMn_2O_4$ is shown in equation 2.4.

$$LiMn_2O_4 \leftrightarrow Li_xMn_2O_{42} + (1-x)Li^{n+} + xe^- \tag{2.4}$$

$LiCoO_2$

This material can be synthesized by mixing cobalt oxide or cobalt carbonate with lithium carbonate or lithium hydroxide in a temperature between 700 to 1000°C with theLi:Co ratio of 1:1. The particle fabrication process takes about 1 hour. The capacity of this particle is between 100 to 140 mAh/g [49].

The final material has a hexagonal layered structure with a molar mass of 97.83 g/mol. The higher thermal stability and good reactions make these materials suitable for cathodes of lithium-ion batteries. The voltage range of this material is between 3.5 to 4.3 V [50]. Figure 2.4 shows the crystal structure of this particle.

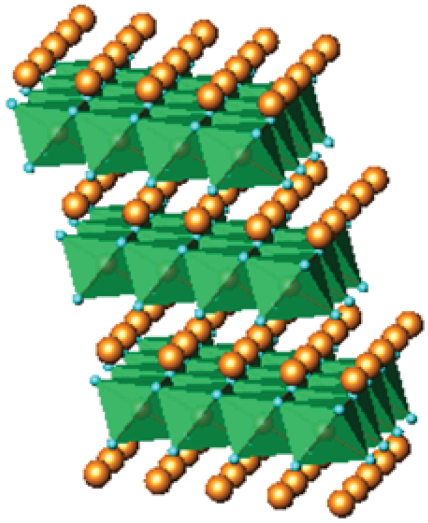

Fig. 2.4. Crystal structure of $LiCoO_2$ [48]

The chemical reaction of $LiCoO_2$ is shown in equation 2.5.

$$LiCoO_2 \leftrightarrow Li_xCoO_2 + (1-x)Li^{n+} + xe^- \tag{2.5}$$

$Li_4Ti_5O_{12}$

The synthesis of this material was started by adding the TiO_2 and Li_2CO_3 with the ratio of Li:Ti for 4:5 to hexane or ethanol. The mixing was done using a ball milling machine and the final product is dried for 12 hours inside an oven with a temperature of 80°C. The product then receives another heat treatment for 2 hours with a temperature between 750 to 900°C [51, 52].

This material has a cubic crystal and can produce the capacity between 100 to 160 mAh/g with the working voltage between 0.5 to 2 V. The most stable voltage for this material is around 1.5 V [52, 53]. Figure 2.5 shows the $Li_4Ti_5O_{12}$ crystal.

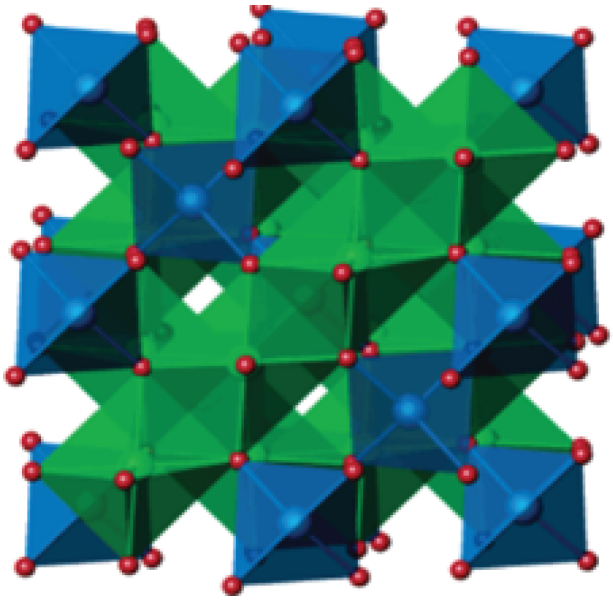

Fig. 2.5. Crystal structure of $Li_4Ti_5O_{12}$ spinel [54]

The chemical reaction of $Li_4Ti_5O_{12}$ is shown in equation 2.6.

$$\mathrm{Li}_4Ti_5O_{12} \leftrightarrow \mathrm{Li}_xTi_5O_{12} + (1\text{-x})\mathrm{Li}^{n+} + xe^- \tag{2.6}$$

Furthermore, table 2.1 shows the other cathode and anode materials for lithium-ion batteries.

Table 2.1
Anode and cathode materials for lithium-ion batteries

	Name of the salt	Formula
Anode	Lithium cobalt(III) oxide	$LiCoO_2$
	Lithium iron(III) oxide	$LiFeO_2$
	Lithium manganese oxide spinel	$LiMn_2O_4$
	Lithium manganese dioxide	$LiMnO_2$
	Lithium nickel dioxide	$LiNiO_2$
Cathode	Lithium titanate	Li_2TiO_3
	Lithium titanate spinel	$Li_4Ti_5O_{12}$
	Lithium metal	Li
	Carbon	C
	Tin(IV) oxide	SnO_2

2.1.2 Electrolyte

An ionic conductive material that can transfer lithium ions from one electrode to another is called an electrolyte. The electrolyte for a lithium-ion battery must be non-aqueous to prevent any reactions with lithium materials. There are two types of liquid and solid electrolytes for these batteries. Liquid electrolytes can be an organic or inorganic solvent based and solid electrolytes can be ceramics or polymers based. The rules of electrolytes are shown below [3]:

- The electrolyte must be aprotic so there are no hydrogen atoms inside the solution.
- The electrolyte should be non-reactive with lithium compounds.
- The ionic conductivity of the electrolyte must be high.

- It must be ionic conductive at the working temperature of the battery.
- It should meet the safety requirements, such as being non-explosive, having high stability, and being non-toxic.

Liquid organic electrolytes are produced by mixing ionic salts with organic solvents. The salts can be $LiPF_6$, lithium hexafluoroarsenate ($LiAsF_6$), lithium perchlorate ($LiClO_4$), Lithium trifluoromethanesulfonate ($LiCF_3SO_3$) and other salts and the solvents can be ethylene carbonate (EC), diethyl carbonate (DEC) and dimethyl carbonate (DMC) [1, 3]. $LiPF_6$ is one of the general liquid electrolytes in the liquid based cells. This lithium salt can resist voltages up to 5 V so it is very convenient for high voltage cells such as $LiNiPO_4$ [55]. The solvents for these liquid electrolytes are mostly ethylene carbonate (EC) and dimethyl carbonate (DMC). The mixture of these two solvents has a very low electron conductance and it is liquid in room temperature. The inorganic electrolytes are mostly used in liquid cathode non-rechargeable cells. The solvents can be sulfuryl chloride, or thionyl chloride, with the additives such as Potassium chloride (KCl), Bromine monochloride ($BrCl$), Lithium tetrachloroaluminate ($LiAlCl_4$), and Lithium tetrachlorogallate ($LiGaCl_4$) [3, 56]. Table 2.2 is showing different lithium salts that can be used for lithium-ion batteries and table 2.3 shows the solvents.

One of the problems with liquid electrolyte cells is the formation of SEI over the negative electrodes after a few cycles. The SEI layer reduces the durability of the battery and reduces the capacity of the battery. This irreversible reaction in negative electrons causes the formation of a solid layer. This layer is made by the reaction of the electrolyte over the electrode surface and provides a layer of solid electrolyte over the electrodes. This layer increases the internal resistance of the cell and reduces the penetration of the liquid electrolyte through the electrode surface [45].

Table 2.2
Different lithium salts for liquid electrolytes

Name of the salt	Formula	Molar weight (g/mol)	impurities
Lithium hexaflurophosphate	$LiPF_6$	151.9	H_2O , HF
Lithium tetrafluoroborate	$LiPF_4$	93.74	H_2O , HF
Lithium bisoxalatoboratel	$LiB(C_2O_4)_2$	193.7	H_2O
Lithium bistrifluoromethane sulfonimide	$LiN(CF_3SO_2)_2$	286.9	H_2O

Table 2.3
Different solvents for liquid electrolytes

Name of solvent	Boiling point (C°)	Melting point (C°)	Density (g/mol)	Viscosity(cP)	Dielectric constant	Molar weight	Conductivity at 20°C (mS/cm)
Ethylene Carbonate	248	39	1.41	1.86	89.6	88.1	6.9
Diethylene Carbonate	126	-43	0.97	0.75	2.82	118.1	2.9
Propylene carbonate	242	-48	1.21	2.5	64.4	102.1	5.2
Dimethyl carbonate	90	4	1.07	0.59	3.12	90.1	6.5
Ethyl methyl carbonate	109	-55	1	0.65	2.9	104.1	4.3

The solid polymer electrolytes are made by mixing polymers with ionic conductive salts. Polymers like polyethylene oxide (PEO), polyvinylidene fluoride ($PVDF$) or poly(methyl methacrylate) are some of the bases for these electrolytes. These polymers are mixed with salts such as $LiClo_4$, $LiAsF_6$ and bis(trifluoromethane)sulfonimide lithium salt ($LiTFSi$) to make the ionic conductive polymers. These electrolytes are still under research due to their low ionic conductivity and high working temperature [57]. Another type of solid electrolyte is ceramic based. Ceramic electrolytes have been recently developed to make thin film cells and lithium air configuration batteries. The conductivity of these solid electrolytes is higher than polymer based electrolytes but they are non-flexible and hard to produce. $LISICON$, $LICGC$, and $LIPON$ are some of these ceramics [21, 58]. The ionic conductivities of the different electrolytes is shown in figure 2.6.

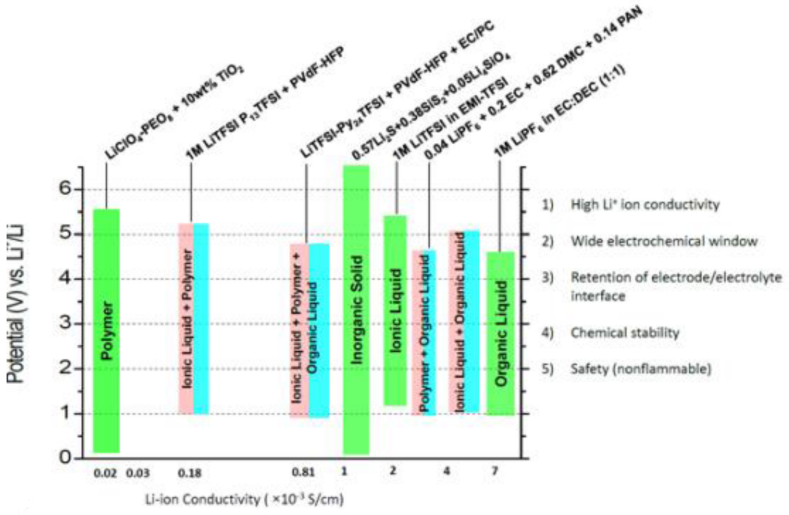

Fig. 2.6. Working voltage vs. ionic conductivity of the different electrolytes [39]

2.1.3 Current collectors

The second main part of the electrode is the current collector section. The layer of active material is in contact with this layer. The main function of the current collector layer is to collect the electrons from or import the electrons to the active material layer. Some of the traditional current collectors for lithium-ion batteries are porous carbon, nickel, aluminum, and copper. The metallic current collectors are suitable for lithium-ion batteries due to their higher conductivity, cost efficiency, and better stability in battery reactions. Commercial lithium-ion batteries mostly use aluminum and copper current collectors for their cathode and anode, respectively [1]. While metallic current collectors are widely used for commercial products, nonmetallic current collectors made by polymers and highly conductive nanoparticles, are growing.

Following are some of the metallic current collectors with their characteristics [3, 40, 59]:

- Aluminum: This metal is widely used for the positive electrode of the lithium-ion cells due to its tolerance in high voltages; it can resist voltages up to 4.3 V without reacting with lithium ions. Because of this stability it is used in many forms from nanolayers to metallic sheets inside different lithium-ion cells with different configurations. Moreover aluminum can protect itself from electrolytes by providing a layer of aluminum oxide over its surface.

- Copper: This metal generally is used for negative electrodes. Current density of this metal is between 0.1 to 1 mA/cm^2. Although this metal is stable in most cases, it reacts with liquid electrolytes made by $LiPF_6$ in EC/DEC in currents above 3.6 V. Nickel or stainless steel are better current collectors for high voltage cells.

- Gold: One of the most stable materials with different reactions inside the cell is gold and it can be stable up to 4 V. The higher price and lower conductivity of this metal in comparison with other metals are the main reasons that it is not widely used.

- Chromium: It is widely used in primary lithium-ion batteries and low voltage cathodes. This metal is more stable than other ordinary electron collectors such as copper and aluminum.

- Silver: Silver is mostly used for positive current collectors. This material is not used as a film, but silver nanoparticles that coat other surfaces, such as carbon, are used as the current collector. Silver electrodes might react with the polyethylene carbonate which is a part of the solvent for liquid electrolyte. In addition to its reaction, using silver is costly, and the conductivity is poor so it is not used widely in lithium-ion batteries.

- Palladium: Palladium is very high intrinsic metal in contact with lithium ions. The only problem with using this metal for lithium-ion batteries is lack of good electrical conductivity.

- Titanium: This metal is another stable material like aluminum. Furthermore, it is not expensive and it can be stable up to 4.5 V. The only negative point of using that in comparison with aluminum is that the corrosion rate of this metal is faster than aluminum.

- Iron: This metal is not stable and in voltages above 1.7 V, it would get dissolved in the electrolyte solution.

- Carbon: Glassy carbon is another material that is used as a current collector. This material is very stable and can tolerate voltages up to 4.5 V. Although this material is very stable, it is fragile, and the conductivity is lower than other metals.

Following are some of the non-metallic current collectors with their characteristics:

- CNT sheets: Carbon nanotubes are widely used in the energy storage devices. This material can provide a good electrical conductivity, and it is stable, although its fabrication process is complex and cost effective [9].
- Silicon: Silicon is another material that can be used both as the current collector and active material. Due to the reactions of this material with lithium-ion, silicon mostly used as the anode electrode [30].
- Polypyrrole: This polymer is used in the cathode of the lithium-ion batteries due to its conductivity, and stability although the conductivity of this polymer is very low comparing to other current collectors [60].
- $PEDOT$: This polymer is conductive but it can be oxidized so fast in contact with air or chemical reactions. This material cannot be used by itself without any protection inside a cell [14].
- Graphite: Graphite based current collectors are made due to their flexibility and conductivity. The only problem of using graphite is that this material can absorb lithium ions and act as an active material by itself so it can change the characteristics of the batteries [61].

Studies show that the aging problems such as capacity degradation and low cyclability of the lithium-ion batteries are related to the degradation of the current collector. Problem such as capacity drop are related to the aggregation of the lithium between the active material and the layer of the current collector. Any impurities or any reactive material over the current collector layer can produce this phenomenon and reduce the quality of the battery in the long term of usage. Corrosion of metallic current collectors is another problem [62]. Furthermore, a research shows that bending of the electrodes can reduce the cycle life of lithium-ion batteries. Increasing the

internal resistance of the current collector is increased by bending and it can reduce the capacity of the lithium-ion battery [9].

2.1.4 Theoritical modeling

Voltage

The potential of a cell can be calculated theoretically by the type of active materials used. This voltage can be calculated from free-energy of the materials. Theatrical free energy is defined by formula 2.7 [3]. Here G is Gibbs energy F is Faraday constant, n is number of electrons and E^0 is standard potential.

$$\Delta G^0 = -nFE^0 \tag{2.7}$$

The voltage of the cell is derived by Nerst equation 2.8 [3]. In this equation T is temperature and R is the gas constant.

$$E = E^0 - \frac{RT}{nF} ln \frac{[ions\, outside\, the\, cell]}{[ions\, inside\, the\, cell]} \tag{2.8}$$

The total voltage of a cell can be driven from oxidation and reduction potential of its chemical reactions.

Impedance

Impedance of a lithium-ion battery is related to the active materials. For different materials, there are different electrical models due to their chemical reactions and stabilities, but for normal materials, there are three impedance sections inside a cell. First, resistance is the interior resistance of the cell related to the resistivity of the

electrolyte materials. Second, there is a capacitance and a resistance related to the charge transfer inside the cell. Finally another capacitance and resistance related to the changes inside the materials, such as SEI formation, must be considered [45].

Figure 2.7 shows a normal model of the cell impedance. R_s in this equation is the resistance of the electrolyte. C_{dl} is double layer capacitance caused by two electrodes and a separator, and R_f is charge transfer resistance. In addition, figure 2.7 shows other impedance which is called Warburg Impedance. This impedance caused by diffusion control and causes a straight line with a 45-degree slope in lower frequencies. A Warburg Impedance element (W) can be difficult to recognize in some models but it can be seen in the many battery applications. W is a semi-infinite linear model for diffusion inside the electrode. This parameter is nearly always associated with a charge-transfer resistance. This parameter can be used to model semi-infinite linear diffusion [3].

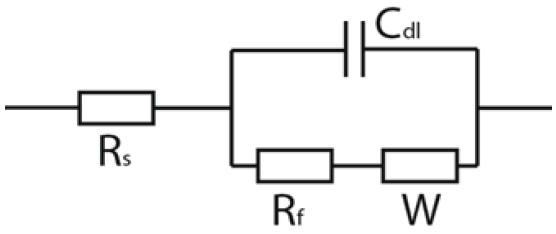

Fig. 2.7. Two stage impedance model of a Lithium-ion cell

To find the impedance of the separator, high frequency tests must be provided. As it is shown in figure 2.8 the higher frequency neglects the effect of C_{dl} and in that case the impedance of the separator can be seen by itself.

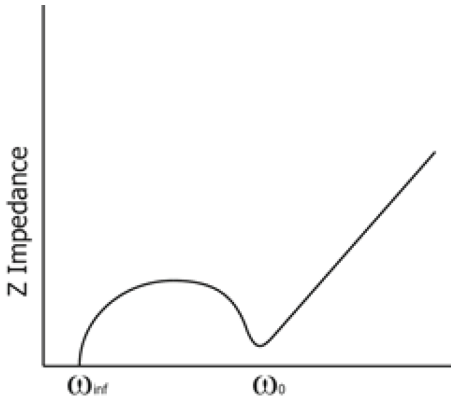

Fig. 2.8. Impedance sample

The impedance can be driven using Eulers formula 2.9, where E is voltage and I is current [3].

$$Z(\omega) = \frac{E}{I} = Z_o exp(j\phi) \tag{2.9}$$

Furthermore, figure 2.8 shows the changes of the impedance inside a lithium-ion battery. As it is apparent in lower frequencies the total impedance is higher than the impedance of the higher frequencies. In higher frequencies there is no time for the cell to act as the capacitor and the only measured impedance is limited to the electrolyte impedance.

The frequency test of the battery can show the R_s and $R_s + R_f$ values. When frequency is infinity the only visible impedance is the resistance of the cell and when the frequency is zero, the visible resistance is the summation of both charge transfer resistance and resistance of electrolyte. The R_s value can be changed by materials inside the cell but as long as this value is low in comparison with the resistance of the electrolyte, and the value of R_f which is 10 times higher than R_s, this value can be neglected. The value of R_f is related to the electrochemical reactions inside the

cell. Equation 2.10 shows the R_f. Here T is temperature, R is material constant, n is number of electrons, F is Faraday Constant and i_0 is exchange current density.

$$R_f = \frac{RT}{nFi_0} \tag{2.10}$$

There are other equivalent circuits for different cells of complex lithium-ion salts. some other examples of these cells are shown in figure 2.9. Each of these cells is made by specific materials and separators. In figure 2.9, the model A can be used for materials such as TiS_2, model B can be used for $LiMn_2O_4$ and model C can be used for $Ni(OH)_2$ or its compounds.

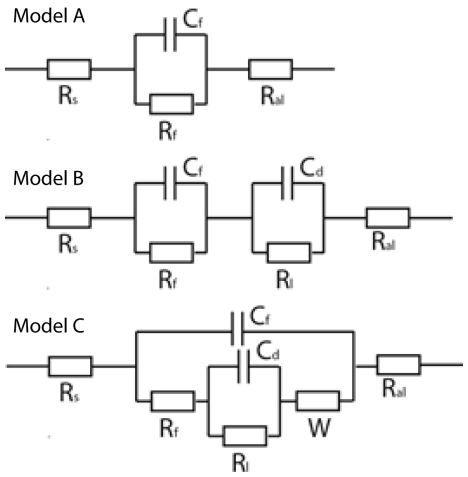

Fig. 2.9. Possible equivalent circuits for Lithium solution interface

Capacity

To calculate the capacity of the battery through an experiment, a galvanostat (amperostat) is needed to measure the load of a cell while keeping its current. The working current, voltage, and charge/discharge time of the cell can be used in calcula-

tion of the capacity of a lithium-ion battery. This device can also detect the changes in cell resistance by changes in the output voltage. From ohms law 2.11:

$$\begin{aligned} R &= U/I \\ I &= U/(R_x + R_{load}) \end{aligned} \tag{2.11}$$

Here U is the measured potential of the cell. In most measuring devices the interior resistance (R_x) is very low so the equation can be written as equation 2.12:

$$I = U/R_{load} \tag{2.12}$$

The power of the cell and the energy then can be derived from the following formulas 2.13:

$$\begin{aligned} P &= U.I \\ W &= P.t \end{aligned} \tag{2.13}$$

Where P is power, W is energy and t is the time of the test. Energy 2.14 can also be driven from the following equation [39]:

$$\begin{aligned} Q &= I.t \\ W &= U.Q \end{aligned} \tag{2.14}$$

2.2 Flexible batteries

Flexible batteries are made with different approaches such as using flexible current collectors, or nano active materials. The regular batteries, due to the nonflexible layers of the active material and the metallic-based current collector are not suitable for flexible applications.

Making a flexible current collector is one of the requirements to produce flexible batteries. Flexible current collector substrate must provide a very low resistance in contact with the active material. Furthermore, this substrate can be bent without losing the layer of active material or its conductivity. A research study shows that the metallic electrodes are not stable for bending due to the loss of conductivity [9] and the loss of the active material layer [25]. Metallic current collectors cannot provide a perfect connection with the active material layer due to the chemical bonding of the polymer binder inside the layer of the active material. This binder is mostly a polymer and its molecules cannot perfectly attach to the metallic surfaces. A flexible current collector must be strong enough to resist through the different forces while it bends. Paper and polymer substrates can provide a better interface with the polymer binder of the active material layer. This makes paper-based and polymer-based current collectors some of the suitable materials for flexible cells. Polymers and paper based materials can provide also better porous structure and higher surface area than regular current collectors. Using polymer based or paper based current collectors are the two main strategies for the fabrication of flexible batteries.

Polymer-based current collectors, can be made by a conductive polymer or a layer of flexible polymer coated with a conductive material. Some conductive polymers such as polypyrrole (PPy), or poly(3,4-ethylendiocythiophene ($PEDOT$) are used to produce the current collectors in some cells such as zinc-Air batteries [8,14]. In a zinc-Air battery a layer of PPy provides the anode current collector, while $PEDOT$ over the paper forms the current collector and the cathode at the same time. In another case, a layer of CNT is provided over polyethylene terephthalate (PET) to produce the current collector surface. The conductivity of this film is about 30 Ω/sq [9].

In paper-based devices, instead of a layer of polymer, highly conductive materials get deposited over the paper substrate using methods such as hot press, printing, and nanocoating. As an example, a CNT ink is provided with silver nanowires and car-

bon nanotubes with a polymer binder. This ink is deposited over the paper to make a conductive layer over the paper. This conductive layer forms a current collector. The conductivity of this paper is 10 Ω/sq [14]. In another experiment, the CNT ink is deposited over the ITO glass, and then after drying, the film is removed from the ITO glass and pressed over the paper to produce the conductive papers while the sheet conductance reaches to 5 Ω/sq [31]. In another approach flexible graphene paper is used as the electron collector which can provide better flexibility and comparable conductivity with the metallic current collectors [63]. The graphene sheet is produced by chemical vapor deposition (CVD). This sheet can work within the voltages between 0.01 to 3 V with $LiPF_6$ liquid electrolyte. The graphene sheet is very stable in chemical reaction inside the lithium-ion battery, flexible due to its crystal structure and it can provide high conductivity [28]. Graphene-wrapped iron(II,III) oxide (Fe_3O_4) anode is another flexible electrode that is made of graphene sheets. In this electrode the grapheme sheet is a substrate for Fe_3O_4 particles. The carbon coated Fe_3O_4 nanowires are inserted into the gaphene layers. The grapheme layer can provide the structural stability for the active materials and act as a binder layer and current collector layer at a same time. The batteries which are made with this method can provide the capacities up to 1025 mAh/g [64].

Metallic-polymer films are another form of the flexible current collectors. These metallic nano electrodes mostly are made by depositing nanowires of metallic rods such as gold over SiO_2 or a $PMMA$ polymer sheet [65]. Other research shows that silicon nanowires can also take the place of the regular active materials of lithium-ion batteries [66]. Materials such as silicon, germanium and tin also can be the anode of lithium-ion batteries, due to their high specific capacity and ionic absorption [66,67]. Forming the Nano rods from these materials can provide an electrode with a large surface area and provide acceptable ionic transportation. Although the voltage and capacity of these cells are still very low (1 to 10 mAh/cm^2) research shows that they can become more efficient in the future due to their low fabrication costs and

high flexibility. Nanostructure carbon based electrode is also another solution for the fabrication of tin flexible batteries. LbL deposition of multiwall carbon nanotubes ($MWNT$) with magnesium oxide or ruthenium(IV) oxide can also provide a thin film battery [68].

In another approach three-dimensional $ZnCo_2O_4$ nanowires are now used as the active material for lithium-ion batteries. This material has a 3D structure and it can produce the capacity in the range of 1300-1400 mAh/g while provide flexibility. In this battery graphite anode is used, but for cathode $ZnCo_2O_4$ nanowires get deposited over the carbon cloth to provide the flexible cathode. The carbon cloth is the current collector of the cell which is integrated into the active material layer [69]. In this electrode, there is no boundary between the active material layer and the current collector. Vanadium oxide is another material that can be used in the flexible electrodes. Thin films of vanadium oxide (V_2O_5) in this method are fabricated by mixing V_2O_5 and multiwall carbon nanotubes ($MWCNT$) to form a flexible sheet that can be act as the cathode. The electrode does not have any current collector and $MWCNT$ particles inside the active material layer are acting as the current collector. The capacity of this material can be reached up to 140 mAh/g for 50 cycles with the voltage range between 2.5 to 4 V [70]. Cobalt(II,III) oxide (CO_3O_4) is another nanomaterial that can form a flexible electrode for lithium-ion batteries. This material can maintain the capacities up to 700 mAh/g. Co_3O_4 can be grown over many surfaces such as silicon or titanium foil. These electrodes are flexible and strong due to their mild growth fabrication process [71].

2.3 Paper-based batteries

Papers are widely used in different energy storage devices due to their porous structure, and high surface area. Paper-based lithium-ion batteries [9], paper based

microfluidic devices for generating power [72], and paper substrates inside polymer cells are some of the examples of using paper for the fabrication of energy storage devices [31]. In addition, high absorption of the paper makes it a perfect substrate for printable energy storage devices.

Papers can be used in different parts of a lithium-ion battery such as separators and current collector sections. The paper based separators are used due to their porous structure and size of the diameter of the cellulose fibers which is in the range of 5-50 μm. These paper based separators are tested with different electrodes with a broad range of voltage. These cells provide a good capacity and cycle life [73]. The paper based separator provides better absorption while the mechanical characteristics of the paper-based are better than regular polypropylenel (PP) separators [74].

The paper-based current collectors can be more flexible than metallic current collectors. These materials can be used for the fabrication of batteries and super capacitors [25]. Furthermore, compared to the plastic substrates of electron collectors, these paper-based current collectors are more flexible while they are lighter and they are more recyclable [31]. The paper based electron collector can be coated with different materials and used in different cells. The only problem with the paper based current collector is the fabrication costs. Depositing CNT is one of the methods to make a highly conductive paper. A CNT paste can be made by mixing $10\%wt$ of sodium dodecylbenzenesulfonate ($SDBS$) with the single wall carbon nanotubes ($SWNT$). This paste can be deposited over stainless steel substrate. The thickness of the film after drying at 80°C becomes about 2 μm and then the film is pressed over the paper to produce a double layer conductive surface. A CNT layer in this structure provide the conductivity while the paper layer provide the flexibility and the stability for the whole structure [31]. In another approach, a highly conductive ink is made by mixing the silver nanowires and an organic polymer such as polyvinylpyrrolidone. This ink can be deposited or printed over a paper substrate to provide a paper-based

conductive surface. The conductivity for the CNT-based ink is about 30 Ω/sq and for Ag-based ink is about 1 Ωsq [9].

LbL is also another method to produce conductive papers. LbL process is a nanoassembly method for depositing thin films of polymers or particles over a substrate using electrostatic forces [39]. Controlling the thickness of layers and being efficient are some of the benefits of this method. LbL of conductive materials over non-conductive substrates is a solution to produce flexible current collectors. In this method Carbon nanotubes or conductive polymers can be deposit over the paper and provide conductive papers. $PEDOT$, which is a conductive polymer, is deposited over the paper fibers. $PEDOT$ can form a layer with the thickness of 30 nm around the fibers and increase the conductivity of the fibers form 10-3 to 10 S/cm [14]. The conductive fibers made are very stable, while their conductivity can be controlled by changing the concentration of the solutions and the time of LbL steps.

A study shows that the amount of the nano conductive material such as CNT or other conductive polymers for ink deposition methods are significantly higher than the amount of conductive materials needed for LbL nanoassembly. Because the amount of material and fabrication costs of ink deposition method are very high this method is not comparable with metallic based cells [1, 25]. LbL deposition of CNT nano rods or other nano particles over paper substrate can be a solution to provide a flexible and efficient non-metallic current collector. In another approach, PPy rods were deposited over the cellulose or wood fibers to make a conductive surface for the lithium-ion batteries electron collectors [75]. Using wood also is investigated for high performance super capacitors. This wooden surface, which is called Porous Wood Carbon Monolith ($m - WCM$) made by depositing the active carbon over the wood fibers using nitric acid ($HNO3$) and potassium hydroxide (KOH) salts. The vapor of these salts can be used to deposit the active carbon over the wood substrate [76].

3. EXPERIMENTAL

3.1 Fabrication of a CNT-coated paper

The CNT-coated microfiber paper is made through LbL nanoassembly of the nanoconductive materials over the wood microfibers. LbL is based on the deposition of materials with opposite charges over the different surfaces. This method can provide simpler and more practical sequential deposition of different materials [11,39,45]. LbL assembly of multilayers of conductive materials which are poly(3,4-ethylenedioxythiophene)-poly(styrenesulfonate) ($PEDOT$-PSS) and carbon nanotubes causes the formation of uniform multilayers of conductive polymers over the wood microfibers. By forming these conductive layers over the wood microfibers, the electrical conductivity of the fibers increases.

The wood microfibers used in LbL fabrication of CNT-microfiber paper is made from beaten, bleached Kraft softwood microfibers (less than 1% lignin and 99% cellulose). These microfibers are press-dried, and wrapped in bundles of 17 x 14 sheets, supplied by International Paper Company (Bastrop, Louisiana). These hollow wood microfibers have a length between 2-3 mm and a diameter between 35-50 μm [25]. The results of the Zetasizer tests of the microfibers show that these fibers have a negative zeta potential. The wood microfiber can absorb the materials with positive zeta potential such as poly(ethyleneimine) (PEI). To release the wood microfibers, a piece of the press-dried fibers are shredded, and soaked in deionized (DI) water for overnight. The mixture then is stirred to separate all the microfibers from each other.

To deposit the layers of conductive material over the wood microfibers, an aqueous dispersion of $PEDOT$-PSS conductive polymer (3 mg/ml) and CNT (25 $\mu g/ml$) are

used as the anionic components, while PEI (3 mg/ml) is used as cationic polyelectrolyte component. To produce the aqueous dispersion of PEI and $PEDOT\text{-}PSS$, these materials need to be diluted in DI water. The wood microfibers are dispersed inside the aqueous solutions of different materials of each layer and are soaked for couple of times. After that, the wood microfibers are washed with DI water to remove the clumps and residues of the particles from fibers. The fibers are soaked in other solutions correspondingly. The wood microfibers are coated with two bilayers of (PEI/PSS) in the first step to provide a uniform substrate for the next bilayers over the paper fibers. In the next step by coating the microfibers with another two bilayers of ($PEI/PEDOT\text{-}PSS$) and (PEI/CNT) the desired conductivity is achieved. PEI which is a positively charged material serves as a glue to absorb negatively charged compounds. During the LbL process the potential must be above 30 mV to provide better colloidal stability [39].

The conductive sheets were made through an in-house setup made in accordance to the Technical Association of Pulp and Paper ($TAAPI$) T 205T standard to be used as the current collectors [25]. The coated microfibers are weighted and dispersed in DI water again to form the sheets of paper. The mixture is then passed through a high pressure circular filter to collect the fibers uniformly as a sheet. The target weigh of the paper is about 200 g/m^2. At the end the paper sheets are rolled, pressed and finally heated dried for overnight inside the vacuum oven.

3.2 Electrodes

Active materials must be coated over a conductive surface to act as an electrode. This conductive surface, which is called current collector, can be made from metallic sheets, conductive polymers, or other highly conductive substrates. To make the crystals of active material attached to a surface, a binder must be mixed with the

lithium salts and deposited over the current collector. The pastes of binder and active materials are deposited over the current collector using different methods such as blade coating or spray method, and form electrodes.

Binder is mostly an ionic conductive polymer like $PVDF$ which is dissolvable in a solvent such as acetone, ethanol, or n-methyl-2 pyrrolidone (NMP). This binder can produce enough adhesion between the particles and the conductive surface whereas it can transfer ions from interior layers of the active material layer to the outer surface. All the electrodes which aree investigated in thesis are fabricated using $PVDF$ binder with NMP solvent. NMP is widely used due to having a low boiling point, being non-reactive in contact with the conductive microfiber paper, and being a better solvent for binder. Lithium salts are the main materials of each electrode. To have a complete active material paste, some highly conductive particles such as carbon black, Super P Carbon, Super P Lithium (from Timcal) or KS_6 must be added to the solution active material. These highly conductive materials increase the conductivity of the active material layer and transfer the electron from middle layers to the current collector. These can also produce different conductive layers between the active materials. Super P Carbon or Lithium is highly conductive carbon compound whit the particle size of about 40 nm while KS_6 is a graphite compound with around 1 to 3 μm size. Super P is used to provide particle to particle connection, electrolyte abortion and dispersed in the binder. KS_6 also can provide larger conductive paths with porous structure [77]. Other highly conductive materials which are not reacting with lithium and their particle size are in nano or some micro meter could be used as well such as carbon black, or graphite [3].

The paste of electrodes for all the experiments are prepared by 75-85% of active material ($Li_4Ti_5O_{12}$,$LiCoO_2$,$LiMn_2O_4$), 15-10% of highly conductive particles (Super P Lithium and KS_6) and 5% of binder ($PVDF$). Although in first samples the amount of binder is about 10% using spray coating method in conjunction of paper

based current collectors let us to reduce the amount of binder to 5%. Before starting the mixing process the materials get completely dried. $PVDF$ powder is dried inside a vacuum oven for 2-3 hours with the temperature of 50°C. After this step the $PVDF$ power needs to be cooled down and transferred to the mix solution to prevent absorbing moisture.

All the materials of electrode paste are mixed and grinded, before adding the NMP solvent. This solvent dissolves the $PVDF$ and improves the adherence of the electrode materials. This mixture needs to stir for overnight to become completely uniform. Overnight stirring is needed due to the low dissolution rate of $PVDF$ in the solvent. The final paste is coated over the current collector films with spray coating and blade coating methods. Although blade coating is a common method of making electrodes, spray coating can produce better results. Spray coating is using lower amount of binder in the paste mixture. Furthermore, this method can also provide thinner and more efficient electrodes. The thickness of the active material layer is related to the number of sprays over the substrate and the concentration of the solution. The paste the concentration of 150 mg/ml and sprayed over each electrode. It is better to warm up the current collectors before spraying. This can improve the quality of the active material film and prevent fractures. To speed up the drying process and to prevent the trapping of water molecules in the layers of electrodes, after each spray, the electrode must be dried inside a vacuum oven with the temperature between 80-90°C. Over spraying or making the layers tick can causes the fracture in the structure of the active material layer. The maximum thickness of the active material layer reaches to 50 μm. The electrodes then dry inside a vacuum oven for 12 hours with the temperature from 80 to 90°C. After drying process the electrodes must be rest inside the vacuum oven for cool down process. Polymer binder can absorb moisture when it is warm and reduce the quality of the electrode. This drying process in necessary to remove the solvent and water particles from the electrode [25].

3.3 Battery assembly

The schematic of the full-cell paper based battery configuration is shown in figure 3.1. The cell must be assembled inside an argon filled glove box to prevent any damages to the electrodes and electrolytes. The CNT-microfiber paper, and metallic films made by copper and aluminum coated with same paste made by lithium titanium oxide (LTO), lithium cobalt oxide (LCO), and lithium manganese oxide (LMO) with similar concentrations are cut in circular samples with diameter of 0.58 cm, which form the anode and cathode of the developed battery. The electrodes are stayed inside a vacuum oven with temperature of 90°C for 24 hours to become completely dried and then transferred to the golvebox. A Celgard PP separator film divides the anode and cathode of the battery. In half-cell configuration an LTO, LCO, or LMO electrode, a separator and lithium foil (purchased form Sigma Aldrich) which is cut in a circular form with the diameter of 10 cm, are encapsulated, while in full cell configuration two different electrodes are encapsulated with a layer of separator in between of them. The outer surfaces of the CNT-microfiber current collectors are connected to the output of the battery. The positive electrode is directly connected to the outer shell of the coin cell while the negative electrode is connected to the other side of the shell using the stainless still spacer and a spring or nickel foam. The battery assembly is soaked in $LiPF_6$ 1M in an EC/DEC electrolyte solution (1:1 by volume, purchased from Novolyte), pressed, and encapsulated in a coin cell. The CR2016 coin cell configuration with a stainless steel spacer, nickel foam and spring are used to produce paper based lithium-ion batteries. This standard is for stainless steel cases of lithium coin cells with the size of 20 mm diameter 1.6 mm of height. The fabricated coin cell is kept undisturbed for 24 hours allowing it to reach stable states by completely soaking the electrode materials and the separator with the electrolyte solution.

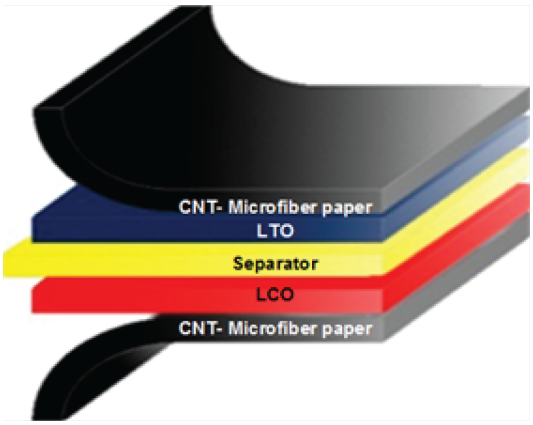

Fig. 3.1. Schematic of the full-cell paper based battery

3.4 Testing

After assembly, the devices are kept undisturbed for 24 hours allowing them to reach stable states by completely soaking the electrode materials and the separator with the electrolyte solution. LCO/LTO half-cells and full-cells are tested using an Arbin BT2000 battery testing system [25]. Arbin BT2000 is a potentiostat and a galvanostat which can control both voltage and current for all testing procedures. This device can control the testing process using predesigned software so primary and secondary cells can be tested using this device with specific procedures [78]. The safety values also must be set before each test. The maximum voltage must be set to 5 V because normally the lithium-ion batteries cannot reach to the voltages higher than that. The current also must be set and there is a short circuit detection circuit inside the testing device to prevent the blast of the cell due to the high currents causes by short circuits. The temperature of the cell must be measured all the time to prevent any dangerous chemical reactions. This temperature must not go beyond 70°C in charging and discharging process and 50°C in rest sections. Temperatures above 100°C can cause damages to the electrodes and separators, while after 130°C thermal runway can accrue [3].

Two types of experiments were conducted for these cells. The first type of experiment is the galvanostatic charge/discharge test and the second type is the self-discharge tests. From galvanostatic charge and discharge experiments the working voltage and current of the testing cell should be set. The voltage is related to the lithium salts were used inside each cell and the current is related to the interiors resistance and time of the experiments. Due to testing the cycle life of the cell, each battery is set to be tested between 15 to 40 cycles to observe the factors such as degradation, short circuit current, and safety issues such as high temperature or explosive reactions. During all of the experiments, the voltage range, the number of cycles, the safety margins and the testing current are set separately regarding to the active materials of each test.

The electrodes are also investigated using two devices. First a micro-probe measurement is done for checking the quality of the paper and electrodes by checking the resistance of the fibers, and the CNT-microfiber paper. This measurement can result in finding the exact values of resistance of the fiber. In addition Scanning Electron Microscopy (SEM) is also provided to check the structure of the film of active materials, fractures, penetration of active material inside the paper and quality of the paper. Because the surface of the active material is not conductive enough for SEM, all the SEM samples are coated with a couple of nanometer layer of gold.

4. RESULTS AND DISCUSSIONS

4.1 *CNT*-coated papers

The resistivity of the microfibers is measured after each bilayer coating of *PEI*/-*PEDOT-PSS* and *PEI*/*CNT* in the *LbL* nanoassembly process. The fibers also visually examined to check the quality of the coated layers. The conductivity of individual fibers is measured using Kiethly System and micro-probing station at 5 to 5 V. As expected, results show that resistivity decreased following the addition of each bilayer of *PEI*/*PEDOT-PSS* or *PEI*/*CNT* on the microfibers. It is also perceived that after a slight increase for *PSS*/*PEI* precursor layers, the resistivity of the microfibers decreases exponentially with the addition of *PEI*/*PEDOT-PSS* and *PEI*/*CNT* bilayers. A layer of *PEDOT-PSS* is sandwiched between *CNT* layers. This forms a thin layer, of about 2 to 5 nm, around the fibers and enhances the electrical characteristics by reducing the resistivity of the coated fiber. This is likely due to the electrical paths provided by *PEDOT-PSS*, which forms a continuous conductive network between *CNT* on the surface of the wood microfibers. It has previously been shown that the *PEDOT-PSS* makes conductive joints between *CNT-PSS* smoother by increasing the clusters [14]. The resistance of the fibers is measured separately using a micro-probe measurement station after depositing each layer and it is shown in figure 4.1. The coated fibers are collected after the deposition of each layer and then the fibers get separated and dried. The resistivity of the fibers are measured separately and collected. The mean, minimum and maximum resistivities of the fibers are measured and collected for each deposited bilayer. The measured resistivity of the fibers is 1.92 $k\Omega$-cm. The study of *CNT* and *PEDOT* paper presented in [39] shows the degradation of the *PEDOT* to be less than 10% over 6 months. In addition, as *CNT* is expected to dominate the conductive path,

even though $PEDOT$ is known for oxidation, its effect on the conductivity of the paper is minimal [14, 25]. The CNT layer over the $PEDOT$ can act as a cover and preserve the conductivity of $PEDOT$ and reduce the contact of this material with air. In addition the paper is used inside a completely argon filled coin cells so there is no oxygen in contact with the paper. This can be the reason for having a constant resistance of the papers through all the experiments.

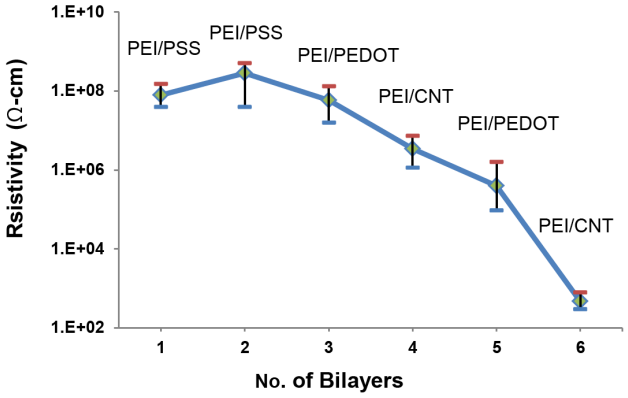

Fig. 4.1. Resistivity of the wood microfibers measured after coating each deposited bilayer of polymer or CNT

A research study is conducted for the washing and depositing process of the CNT-microfiber paper fabrication. In the first study, beside the fibers, the conductivity of a fabricated sheet with the thickness of 50 μm which is used in CNT-microfiber paper current collector is tested. Two different papers, one with made with only a single bilayer of $CNT/PEDOT$ and another one with double bilayers of $CNT/PEDOT$ are fabricated while the other fabrication process remains same. The measured resistivity of these papers with the size of 3 cm^2 and thickness of 100 μm are shown in figure 4.2. It is observed that the resistivity of the paper is improved up to 10 times by adding another bilayer of highly conductive materials. The resistivity of the paper is improved from 11.5 $k\Omega$-cm to 1.5 $k\Omega$-cm.

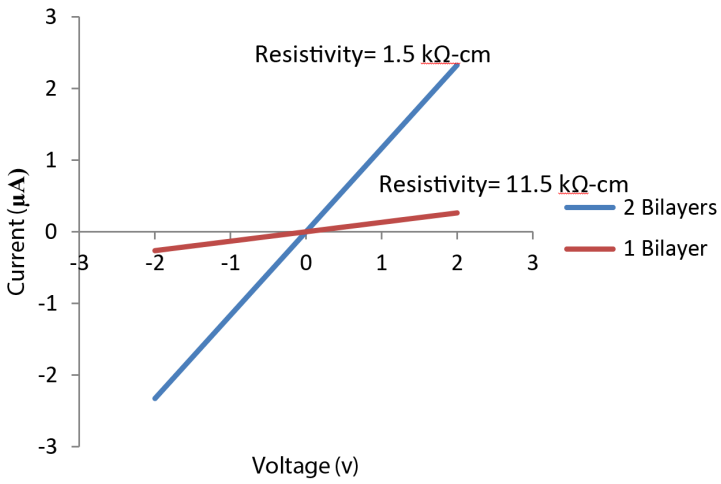

Fig. 4.2. Resistivity of a CNT-microfiber paper sample with different layers

Another study is conducted to investigate the washing procedure of the paper making process. Two papers are made with 2 bilayers of $CNT/PEDOT$, with two different washing processes after each LbL step. One is made using the water jet wash and another one with soaking wash. In the water jet method, the microfibers are washed using a high pressure water jet for 1 minute and rinsed for another 1 minute. In another experiment the microfibers are soaked in DI water for two minutes and then rinsed for 20-30 seconds. The results show that the soaking method is more effective while it can reduce the clumps and residues without damaging the fabricated layers around the microfibers. Figure 4.3 shows the resistance of the CNT-microfiber paper made by these two methods. The resistivity of the CNT-microfiber paper reduces around 3 times by using soaking wash method. The resistivity is changed from 1.5 $k\Omega$-cm to 0.6 $k\Omega$-cm. It shows that the particles are very sensitive to outer pressure before coating the next layer. After coating the next layer, the previous layers are preserved by the new layers.

SEM images of the uncoated and coated microfibers reveal that the surface structures, as shown in figure 4.4. Figure 4.4(a) shows the surface of an uncoated mi-

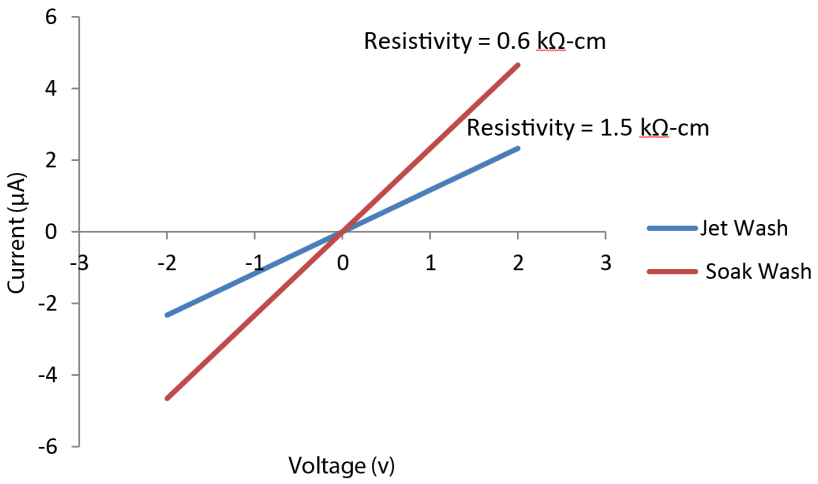

Fig. 4.3. Resistivity of a CNT-microfiber paper sample with different washing methods

crofiber, while figure 4.4(b) shows the surface of a microfiber coated with two bilayers of (PEI/CNT) in alternate with one bilayer of $(PEI/PEDOT\text{-}PSS)$. After forming a sheet with these fibers, the sheet is investigated. The thickness of the paper sheet is measured to be about 50 μm. Ticker papers are not useful in lithium-ion batteries due to their resistance. The resistivity of a CNT-microfiber paper sheet fabricated from these coated wood microfibers is measured to be 1.92 $k\Omega$-cm [25] and can be reach to 0.6 $k\Omega$-cm.

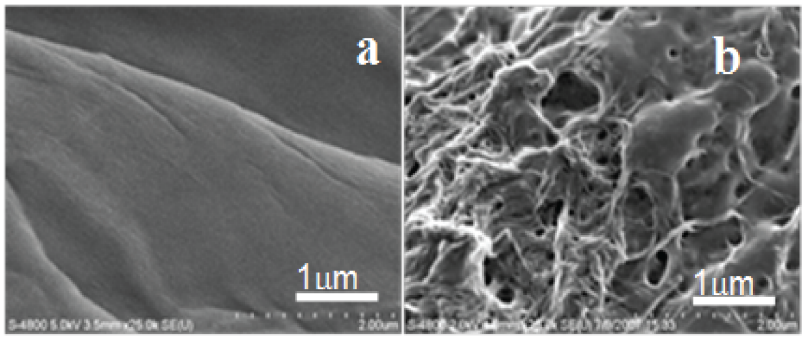

Fig. 4.4. SEM images of (a) uncoated and (b) CNT-coated microfibers [39]

The surface of the electrodes are investigated using SEM images. In this method some used and unused samples are investigated. The used samples are taken from LTO and LCO half-cells. These electrodes are first removed from the cells and lightly washed with the DI water to remove the residue of the liquid electrolyte. Then they are dried for SEM imaging. These samples are coated with gold using evaporation method. The unused electrodes are broken to see the crack formation, paper structure and different layers of active material. Some parts of the active material layer are also removed from the paper current collector. Figure (4.5 to 4.8) shows the formation of active materials over the paper, current collector. The material is drop casted to show the sizes and particles. In this section the quality of the papers and the connection patterns between electrode and current collector fibers are investigated.

The first set of pictures shows the LCO salts (big white crystals) over the fibers. Figure 4.5(a) compares the size of the fibers with the crystal of lithium salt in the middle of the picture and some clumps of the paste materials (super p conductors and binders) on top of the fibers. Although the LCO crystals have different sizes, they are distributed uniformly between CNT-coated fibers. The figure 4.5(b) shows the LCO lithium salt by itself. The figure 4.5(c) is more detailed and shows the fibers from narrower angle. The formations of CNT rods over the fibers are visible in this figure. The smaller lithium salts are also visible in this figure and other conductive and paste materials. The figure 4.5(d) is the cross section of the paper and the formation of the mesh structure with fibers.

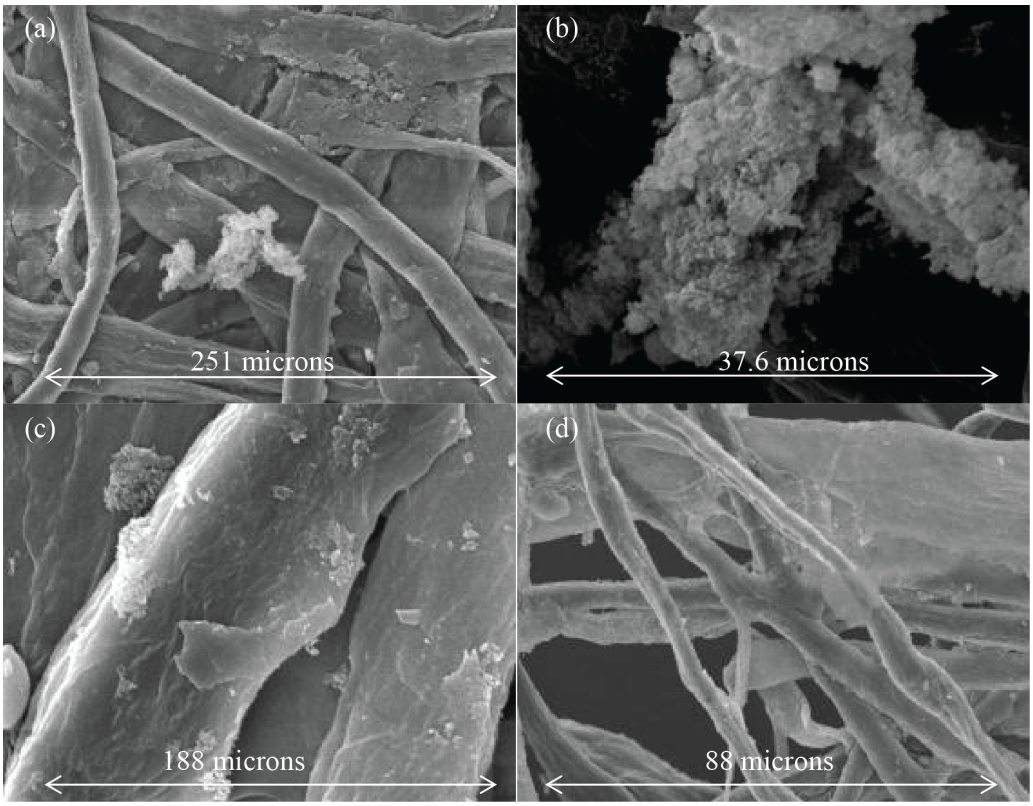

Fig. 4.5. (a) *LCO* salt over the *CNT*-coated microfibers, (b) *LCO* crystal, (c) coated wood microfibers with *CNT* rods, (d) *LCO* coated fibers cross section of fibers

The second sample has the same configuration but uses *LTO*. The *LTO* particles are about 100 *nm*, so the lithium salts in the figures are much smaller. Figure 4.6(a) shows the lithium salt over the fiber. The size of the lithium salt is smaller than the previous device so it needs higher magnification for the clever visualization. For size comparison, this figure contains two lithium salt crystals. The conductive material and binders are visible as clumps on the fibers. Figure 4.6(b) shows the corner of the paper. Again there is enough connection between the fibers. In the bottom part of the picture there are fibers coated with binder and *LTO* and the upper side is *CNT*-coated fibers.

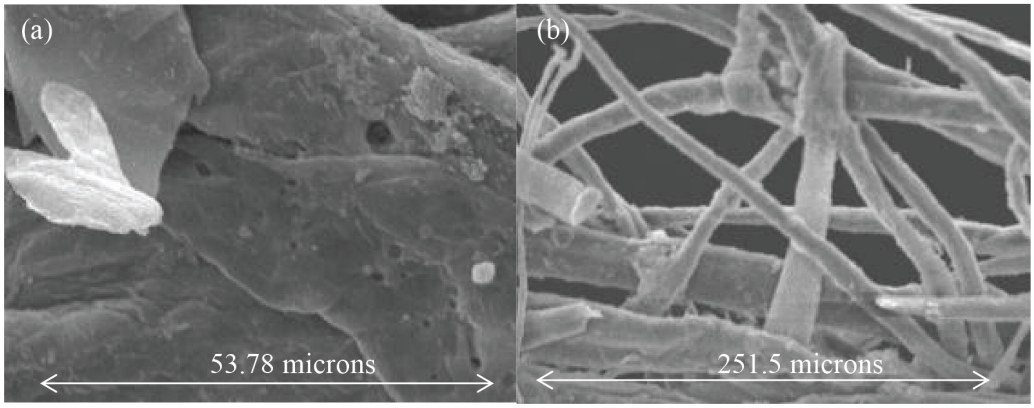

Fig. 4.6. (a) *LTO* crystal over the *CNT*-coated microfibers, (b) *LTO* coated fibers cross section

In the next step, used electrodes are examined. The electrodes are removed from the used full-cells. These electrodes are *CNT*-microfiber paper coated with the active material and used inside a cell for 20 charge/discharge cycles. Figure 4.7(a) shows the used *LCO* electrode. The active material layer is still stable over the surface of *CNT*-microfiber paper. Although there are some fractures over the substrate, these fractures are shallow and contained. These fractures are shown in 4.7(b). The figure shows that the surface is uniform and the structure of the *CNT*-microfiber paper prevents the detachment of the materials. The figure 4.7(c) is the picture of the lithium salt. This is the *LCO* crystal and it is completely connected to the paste material. This is a large crystal and other smaller size crystals can be seen around that. These crystals are covered with the Super P Lithium and form a firm layer. The figure 4.7(d) shows the cross-section of the paper. The upper part is the active material layer and the lower side is the *CNT*-coated fibers. The figure shows that the penetration of the paste into the paper is very limited. Because of that, after drying process of electrodes, the entire paste layer becomes fragile and can get removed from the paper surface.

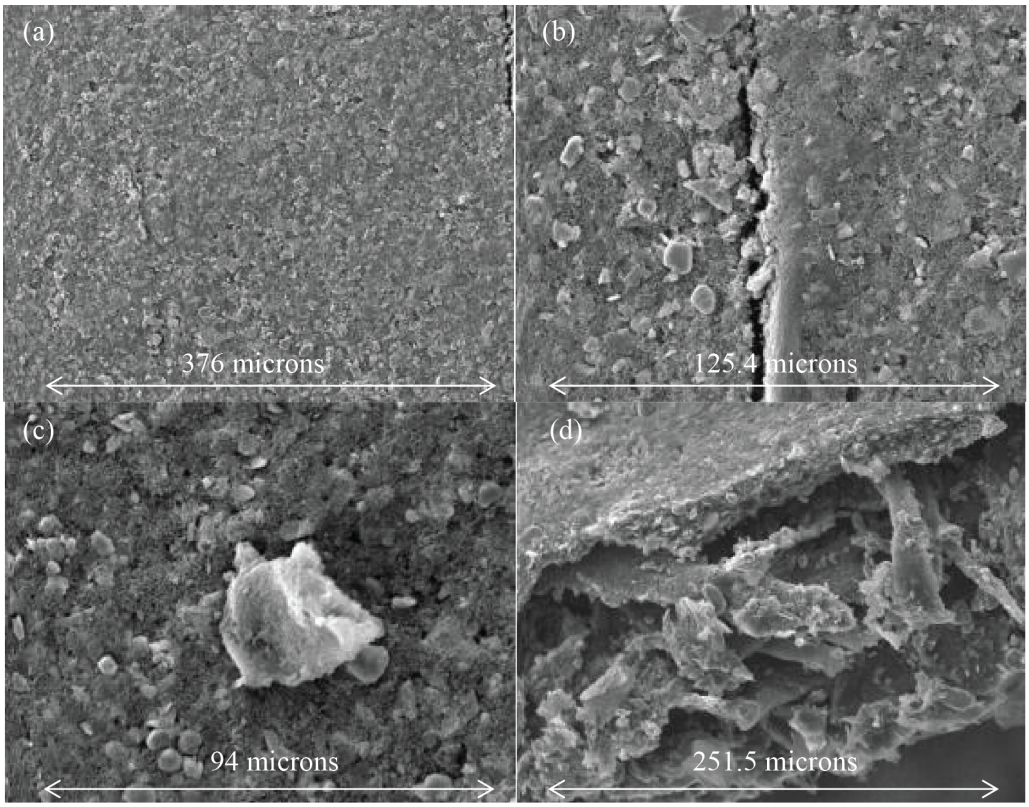

Fig. 4.7. (a)*LCO* electrode surface, (b) fractures over the electrode, (c) *LCO* crystal in comparison with other particles of active material paste, (d) layers of paper and *LCO* active material

The examination of used *LTO* electrode is similar to the *LCO* electrodes. The only difference between the samples is the size of the *LTO* crystals which is smaller than *LCO*. The figure 4.8(a) is the surface of the electrode. The *LTO* crystals are smaller in comparison with the *LCO* crystals inside the active material surface. The figure 4.8(b) shows that the *LCO* electrodes in lower magnification. It seems that the active material layer is thinner than *LCO* electrodes due to the crystal size of the *LTO*. Furthermore, there are some fibers removed from the paper due to the opening of the cell. It seems that the active material got peeled off form the paper fibers after a long charging and discharging process. The figure 4.8(c) also shows that the structure of the paper is not changed after charge and discharge cycles. Figure 4.8(d) shows the cross-section of the paper. Like the previous electrode, penetration

of the active material is limited. The layer of active material covers the surface of the electrode but it is not reached into the middle layers of the CNT-microfiber paper.

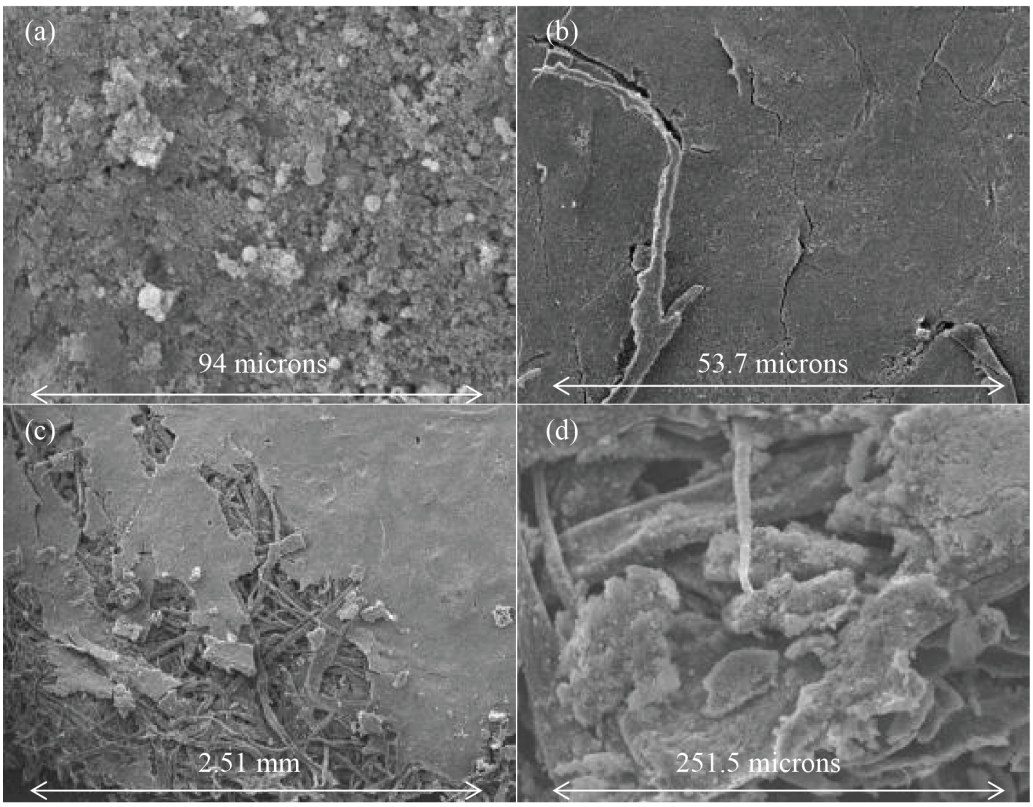

Fig. 4.8. (a) LTO electrode surface, (b) fibers and fractures over the LTO electrode, (c) Removing active material layer form the CNT-microfiber paper, (d) layers of paper and LTO active material

Cross-sectional SEM images of the LCO and LTO coating on CNT-microfiber paper current collectors are presented in figure 4.9, As shown, the electrode material layers (LTO and LCO) that consist of active materials, $PVDF$, and Super P Lithium, form a solid layer on the top of current collectors. It can also be noted that the CNT-microfiber paper current collector and electrode material layers are discrete with some interpenetration. The latter helps the electrode material layers to be intact on the surface of the developed CNT-microfiber paper current collectors [25].

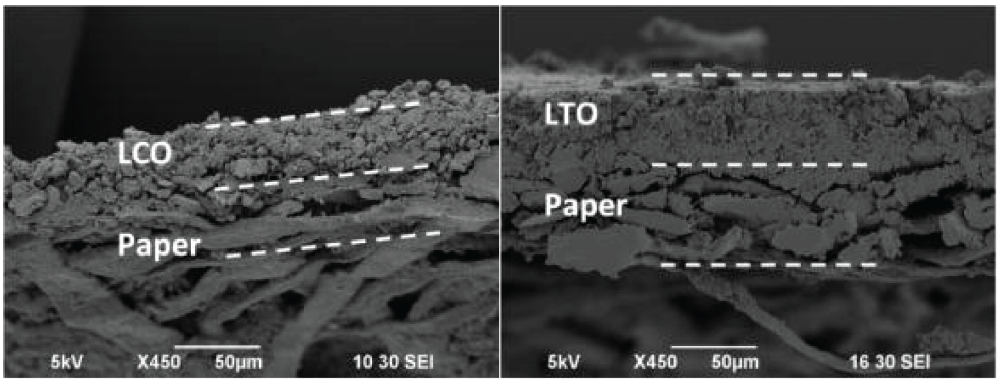

Fig. 4.9. *SEM* images are showing the cross section of *LCO* and *LTO* layers on *CNT*-microfiber paper current collectors

Figure 4.10 shows the higher magnification of the cross section area. It shows that the penetration is very limited and the connection between the porous structure of the paper to the electrode material is higher than a regular aluminum film. This connection is due to the 3D structure of the fibers and their mesh structure. This layer of paper can provide structural stability for the electrodes. Fibers of the paper merge into each other and they are connected to the active material using binder. This can provide better stability and prevent the huge increase in internal resistance of the lithium-ion battery after bending.

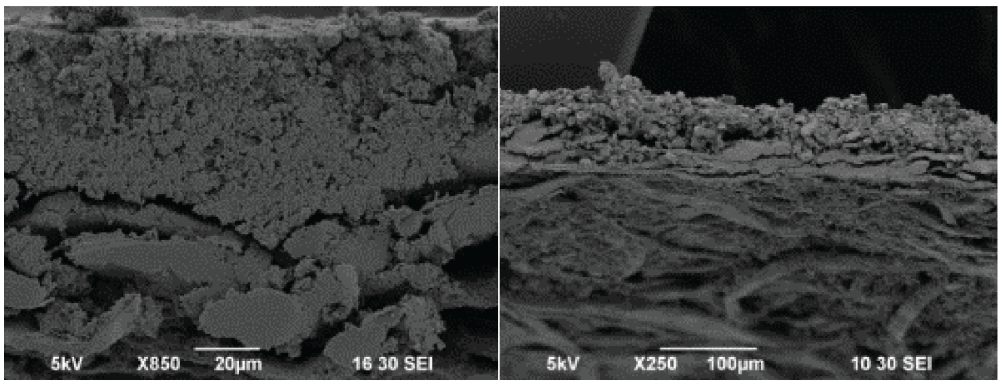

Fig. 4.10. *SEM* image of electrode cross section

The developed paper-based batteries have an inherent flexibility. Literature studies show that the regular metallic current collectors are not flexible due to the low connection between the active material layer and metallic surface. Therefore, the performance under conditions of repeated bending was studied. In this study, LCO and LTO paste are coated on two separate CNT-microfiber paper and metallic current collector samples using spray method with $PVDF$ binder. After vacuum-drying the samples for 12 hours, the fabricated electrodes are bent to a 300° angle 20 times. Then SEM image is taken from each electrode. The SEM images of the resulting samples are shown in figure 4.11(a) (LCO) and 4.11(b) (LTO). For comparison, a similar test is conducted on samples prepared from LTO over aluminum and LCO over copper foils. These SEM images are shown in figure 4.11(c) (LCO on Al) and 4.11(d) (LTO on Cu). The insets of the figures highlight areas with observed surface fractures. SEM images reveal that the electrode material layers on Al and Cu foils suffer from deep fractures over large areas. In comparison, fractures on newly developed microfiber current collectors are shallow and contained. Furthermore, some parts of the active materials over the Al and Cu foils are detached from the surface, introducing gaps under the active material layer. In contrast, no such effects were observed with CNT-microfiber paper current collectors. Although the surface has some fractures, the porous structure of the paper, keeps the material on the substrate, preventing the detachment of active material from the current collector [25].

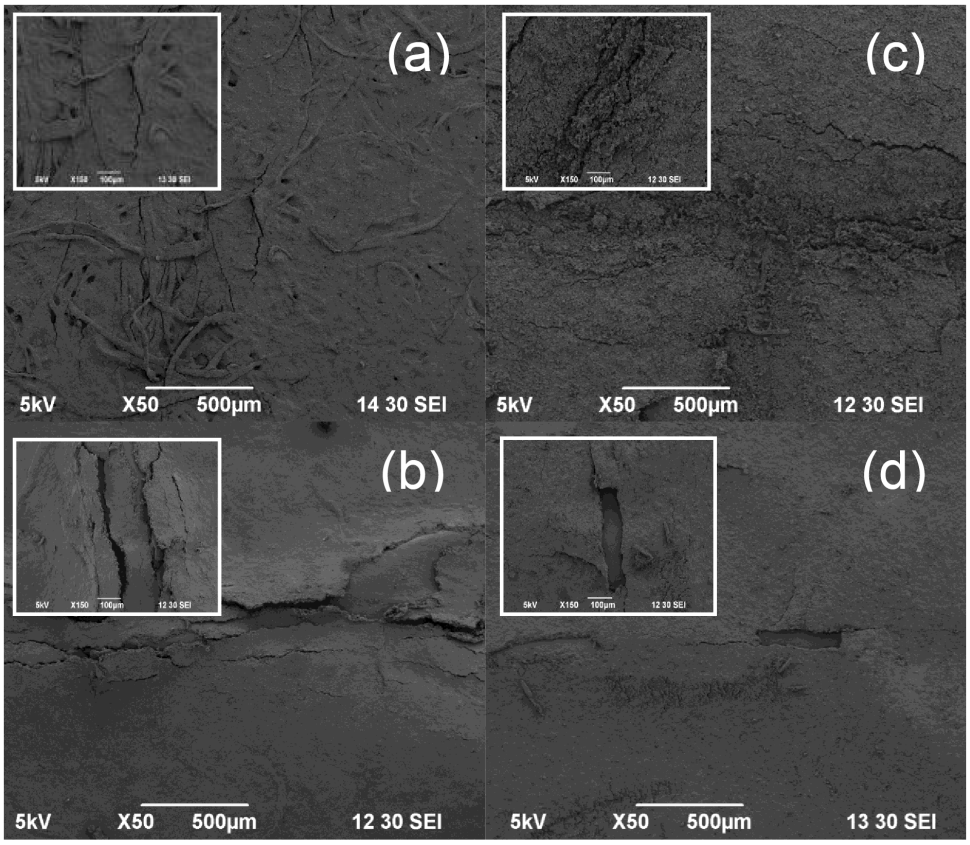

Fig. 4.11. *SEM* images of (a) *LCO* on *CNT*-coated microfiber current collector, (b) *LTO* on *CNT*-coated microfiber current collector, (c) *LCO* on Aluminum foil, and (d) *LTO* on Copper foil. These samples were bent to a 300° angle for 20 times on *CNT*-microfiber paper current collectors

4.2 Half-cells

4.2.1 *LTO*

Standard *LTO* half-cell using *Cu* and *CNT*-microfiber paper current collectors were tested between 0.5 V to 1.8 V. It was observed that the discharging capacity of the metallic based current collector *LTO* half-cell is 156 mAh/g at $C/5$. Respectively, the capacity of *CNT*-microfiber paper current collector *LTO* half-cell is observed 158 mAh/g at $C/5$ current rate. The charging/discharging capacity curves *LTO* half-cells is shown in figure 4.12. The mass loading of the active materials on the anode (*LTO*)

was 8.8 mg/cm^2 on both metallic and CNT-microfiber current collectors. The CNT mass loading on CNT-based current collectors is 10.1 $\mu g/cm^2$. The observed capacity of LTO paper-based half-cells is comparable with the equivalent device fabricated from metallic current collectors and tested under the same conditions. The results show the developed cells are stable with a less than 1% drop in capacity from the first to the fifteenth cycle, while the charging/discharging curve patterns are steady.

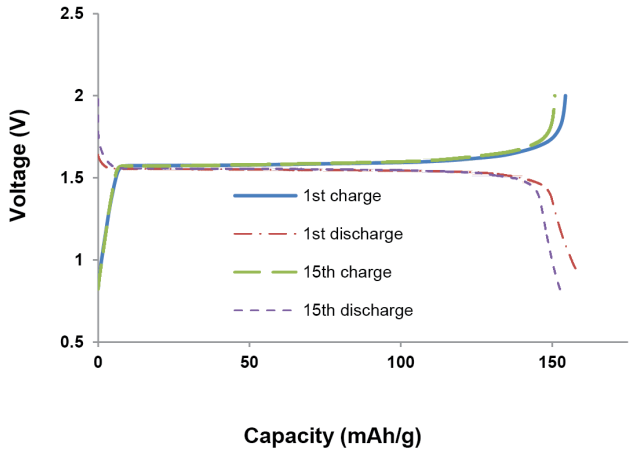

Fig. 4.12. Galvanostatic charging/discharging curves of the 1^{st} and 15^{th} cycles of a LTO half-cells made of CNT-microfiber paper current collectors

To check the quality of the cell, the same experiment is done with a metallic based current collector coated with LTO. Figure 4.13 shows the galvanostatic charging/discharging curves for the same LTO half-cell using the copper current collector. The capacity of this cell is comparable with the paper-based half-cell made with the CNT-microfiber paper. Both capacity and charging/discharging curves are compatible with the paper-based cells.

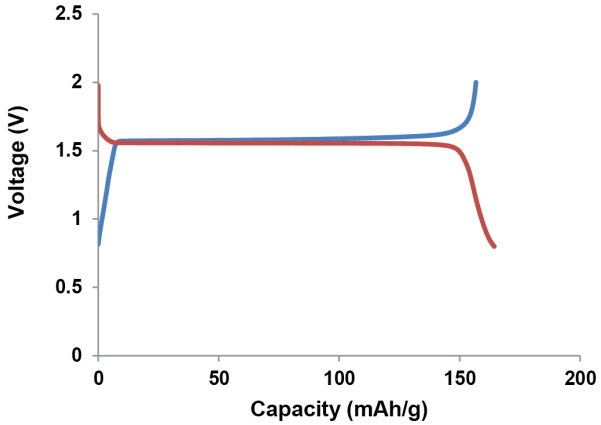

Fig. 4.13. Galvanostatic charging/discharging curves of a LTO half-cells made of copper current collectors

Comparing the results with aluminum and copper foils, shows that the CNT paper, can act as an electron collector, and it can be used to have same capacity of the aluminum and copper materials. In addition, the porous structure of the paper can help contact between the active materials while providing higher surface area for conductive materials, leading to an acceptable capacity and working area.

4.2.2 *LCO*

Standard LCO half-cells using Al current collectors and CNT-microfiber paper collectors are tested between 3.5 V to 4.3 V. It is observed that the charging capacity of the metallic based the LCO half-cell is 149 mAh/g while the charging capacity of paper based half-cell is 150 mAh/g at $C/5$. Figure 4.14 shows the galvanostatic charge and discharge curves of the first and fifteenth cycles of the paper-based half-cell. Observed capacity for the paper-based cell is comparable with the equivalent device fabricated from a metallic current collector while the testing conditions are the

same. The drop in capacity after 15 cycles is less that 1% and the half-cells are stable. The mass loading of the active materials over the LCO electrode is 9.2 mg/cm^2 for both metallic and CNT-microfiber current collectors. The CNT mass loading of CNT-based current collectors for LCO electrodes is same as LTO electrodes which was 10.1 $\mu g/cm^2$. The maximum charging voltage of LCO is set to 4.3 V to ensure reliability of cycling performance and safety margin [50]. Charging LCO over 4.3 V could increase the chance of overcharging and degradation of the electrodes. A comparison between first and fifteenth cycles shows that the pattern is stable and the curves are similar.

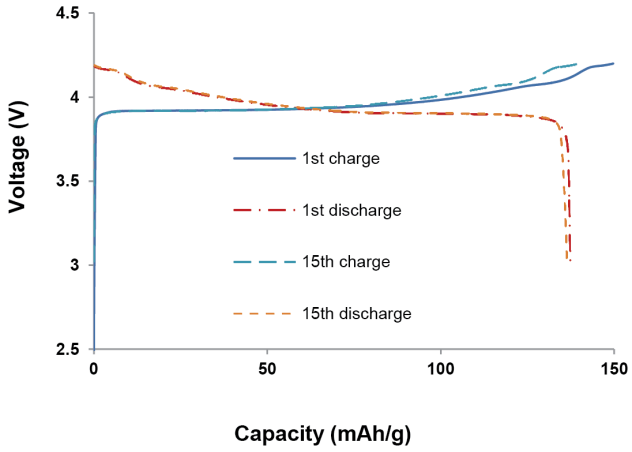

Fig. 4.14. Galvanostatic charging/discharging curves of the 1^{st} and 15^{th} cycles of a LCO half-cells made of CNT-microfiber paper current collectors

The same experiment is done with a metallic based current collector. Figure 4.15 shows the galvanostatic charging/discharging curves for the same LCO half-cell using the aluminum current collector. The capacity of this cell is comparable with the paper based half-cell made with the CNT-microfiber paper.

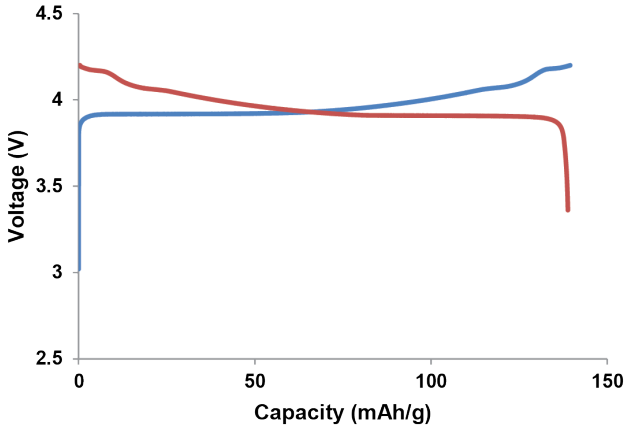

Fig. 4.15. Galvanostatic charging/discharging curves of a *LCO* half-cells made of aluminum current collectors

4.2.3 *LMO*

For the lithium manganese oxide standard half-cells are made using aluminum and paper-based current collectors. The half-cells are charged between 2.5 V to 4.5 V at a 0.2 mA current rate. The galvanostatic charging/discharging capacity results for the paper based and an aluminum current collector half-cells, measured separately, are shown in figure 4.16 and 4.17, respectively. The results show that the performance of the paper-based current collector is comparable with the aluminum based device. The results from both the measurements are compared and the charge capacity of the paper-based half-cell is measured to be 130mAh/g and for aluminum based half-cell it is measured to be 129.5 mAh/g. The charge/discharge pattern and capacity of the metallic and paper-based cells are comparable and in the same range.

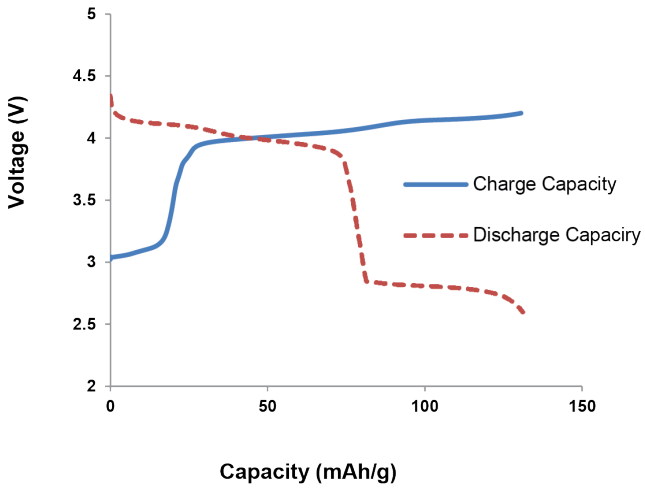

Fig. 4.16. Galvanostatic charging/discharging curves of the 1^{st} cycle of a LMO half-cells made of CNT-microfiber paper current collectors

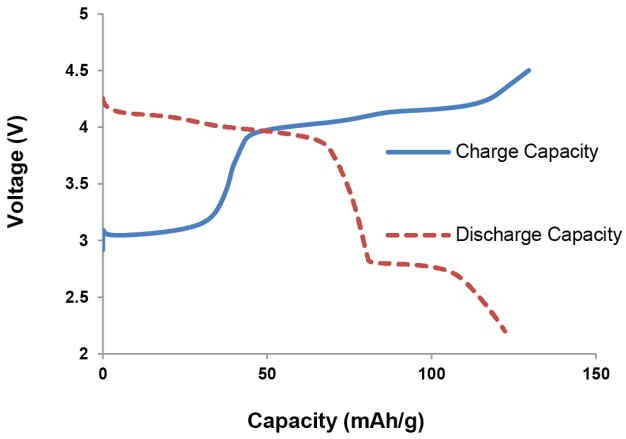

Fig. 4.17. Galvanostatic charging/discharging curves of the 1^{st} cycle of a LMO half-cells made of aluminum current collectors

Table 4.1 shows the comparison between the results of different half-cells. From this section, LTO and LCO are chosen to form a full-cell. The voltage range shows that the paper can be used in this cell by providing a voltage between 1.2 to 3 V.

Table 4.1
Comparison between half-cell results

Lithium salt	LTO	LCO	LMO
Mass Loading (mg/cm^2)	8.8	9.2	8.5
Voltage (V)	0.5-1.8 ($C/5$)	3.5-4.3 ($C/5$)	2.5-44 ($0.2A$)
Capacity (mAh/g) (CNT)	158	150	130
Capacity (mAh/g) (metallic)	156	149	129.5
Degradation	Less than 1% after 15 cycles	Less than 1% after 15 cycles	The test was done for the whole cycle

4.3 Full-cells

The full-cells with LTO and LCO electrodes on CNT-microfiber paper current collectors are tested for charging/discharging performance between 1.2 V and 2.7 V. The galvanostatic charging/discharging curves and capacity are measured. In first attempt the maximum charging and discharging capacities of these batteries are measured to be 21 mAh/g and 16.36 mAh/g, respectively as it is shown in figure 4.18.

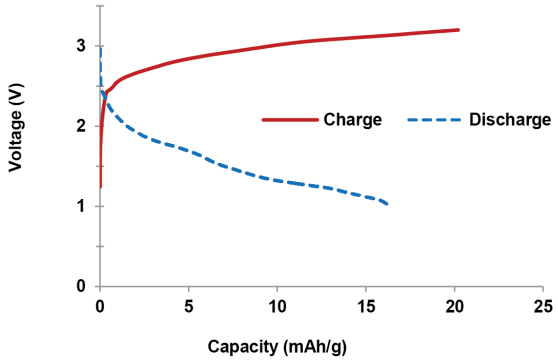

Fig. 4.18. Capacity of the first experiment of LTO/LCO full-cell

The capacity of the first experiment is lower than a regular metallic-based LTO/-LCO full-cell. The further investigations show that the thickness of the current collector for that experiment is more than 100 μm. This can increase the internal resistance of the cell so the capacity can-not reach to its maximum. In addition, the layer of active material is around 100 μm. The optimization process shows that by limiting the thickness of paper, and active material to 50 μm the internal resistance of the cell drops and the capacity can be reached to its maximum. Another optimization process is using spring inside the cell to provide enough pressure. Although the papers are thick enough and it must keep the pressure inside the cell, adding the spring can preserve the pressure during all charge and discharge cycles. The internal resistance of the paper in this experiment is in the 10 Ω level which is comparable with the charge transfer resistance. In this case the battery cannot be charged up to the maximum capacity and it reaches to its maximum voltage sooner. This problem can reduce the maximum capacity and cycle life of the cell [45].

After the optimization process, another set of full-cells is fabricated. The first cycle of this LTO/LCO test is shown in figure 4.19. The maximum charging capacity is measured to be 126 mAh/g at a $C/5$ current rate. Further tests are conducted to check the batteries in higher currents. The tests with higher C rates and the charging capacities are done and the following capacities are measured to 112 mAh/g for $C/2.5$ and 107 mAh/g for C. As the fabricated devices show higher capacity at lower current levels, the batteries are expected to be utilized in low current applications. In lower currents, the effect of the internal resistance of the lithium-ion batteries are negligible and cannot change the capacity of the cell significantly but by increasing the current the batteries reach up to their maximum voltage sooner without providing their maximum capacity. The internal resistance of the cell is more important in higher currents and increases the charging voltage slope. However, further research is in progress to improve the capacity of the devices at higher current levels. The internal resistances of full-cells measured through a Nyquist plot are observed

to be 2.8 Ω for paper-based and 1.95 Ω for metallic current collectors. The CNT current collectors used in the cells constitute a network of cellulose microfibers with porous structures at the micro-scale, and these porous gaps are filled with the applied conductive electrode materials (as can also be seen in the SEM images presented in figure 4.9) reducing the overall internal resistance of the cells as measured by Solarton Analytical Potentiostat/Galvanostat. The energy per mass of the full-cell is observed to be approximately about 302 Wh/g for $C/5$ rate. Table 4.2 shows a comparison between different LTO/LCO cells. As it is shown the maximum capacity can be delivered by the metallic current collectors, while the CNT-based devices are providing acceptable capacity.

Table 4.2
Comparison between different LTO/LCO full-cells

Type of current collector	Voltage range (V)	Capacity (mAh/g)
CNT-microfiber paper	1.2-2.7	126
CNT film	1.5-2.7	130
Metallic	1.2-2.8	208

It was also observed that, after 25 cycles, the charging capacity of the batteries dropped by approximately 15%, mostly caused by the drop at the first charging cycle. The drop in capacity could be attributed to material stabilization, SEI formation, and state of charge/rate capabilities. In a full-cell, the capacity ratio of both anode and cathode electrode materials must be balanced using mass loadings to have the optimum performance. The desired mass ratio for electrodes depends on the amount of cyclable lithium (amount of lithium that can cycle reversibly) and their columbic capacities. The deviation in the actual electrode mass loadings on anode and cathode in a fabricated device due to experimental errors affect the accuracy of the optimized mass balancing. Further, in the first charging cycle, the lithium ions intercalated

into the anode forms side reactions, and also due to secondary processes such as SEI formation results in irreversibly embedded lithium ions into the anode. The formation of SEI over the anode is faster in the first few charging/discharging cycles of lithium-ion batteries. After first cycles the formation of SEI layer become slower and the capacity becomes steady [45, 79]. Therefore, a lower amount of lithium ions are intercalated back to cathode in the first discharge which causes capacity fade for the following cycles [45, 79]. However, in the half-cells, lithium foil provides sufficient ion insertion preventing any deficiency in the following discharge cycles.

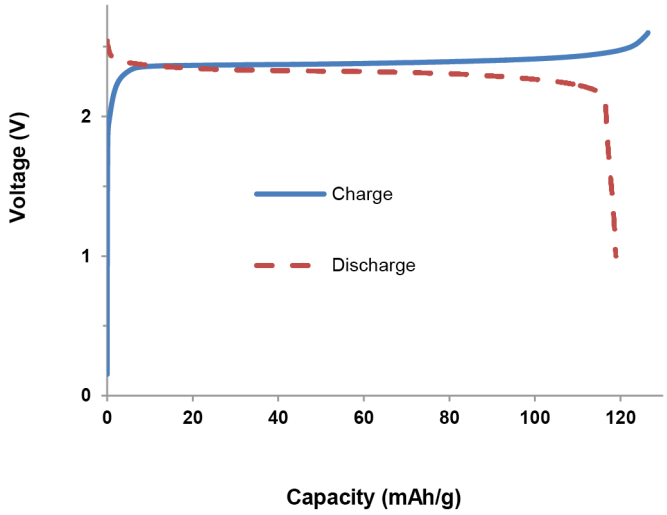

Fig. 4.19. Galvanostatic charging and discharging curves of the LTO/LCO full-cell first cycle between 0 V and 2.7 V

The columbic efficiency of the battery, as shown in figure 4.20, is measured to be 84% for the first cycle, which increases to 96% in the second cycle and stays between 96 98% thereafter. This is attributed to the fact that in the first cycle the charging takes place between 0.2 V and 2.7 V while in the following cycles the discharge voltage is limited to 1 V, resulting in a higher charging time and lower discharging time in the first cycle. In addition, inside a cell there is a small amount of lithium which is

not cyclable and in calculation it is not considered. In the first charging, cycle these ions are trapped inside the electrode or form a layer of SEI over the anode, so the discharge capacity is lower than the charge capacity in the first cycles. In the next cycles, this phenomenon is less noticeable due to the stability of the battery. After the first cycle, the battery reaches its stable state by reducing the speed of SEI formation and balancing the capacity of anode and cathode. At this stage the columbic efficiency is increased and the charge/discharge capacities become more similar to the previous charge/discharge cycles.

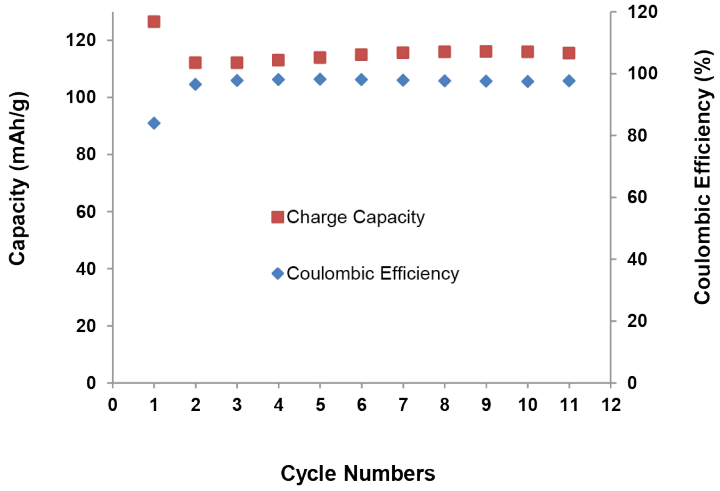

Fig. 4.20. Cycling performance of the LTO/LCO full-cell

Self-discharge results of the full-cell charged to 2.7 V at $C/5$ current rate is shown in figure 4.21. It can be noted that after 90 hours the battery output voltage was stable at 2 V [25].

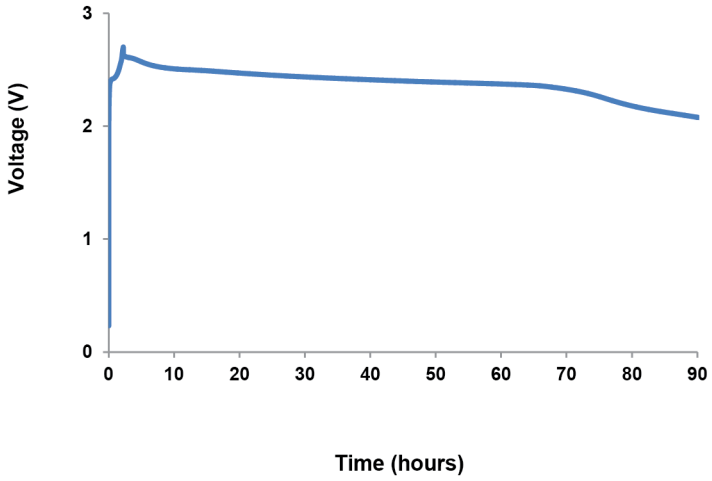

Fig. 4.21. Self-discharging behavior of the full-cell after being charged to 2.7 V

It should be noted that CNT mass loading for the paper current collectors presented in this paper is 10.1 $\mu g/cm^2$, which is 20 times less than CNT current collectors. The capacity of the presented battery in terms of CNT loading is 35.2 Ah/g_{CNT} which is 245% more than previously reported lithium-ion batteries using CNT current collectors [9, 31].

5. CONCLUSIONS AND FUTURE RECOMMENDATIONS

5.1 Conclusions

Flexible and light-weight lithium-ion batteries with CNT-microfiber paper-based current collectors have been studied. In these novel current collectors, wood microfibers were coated individually with layers of CNT through an electrostatic LbL nanoassembly process. The LbL process can keep the characteristics of the fiber while significantly reducing the amount of CNT usage. The CNT-microfiber paper then is used as the current collector of various lithium ion batteries. The characteristics such as capacity, cycle life, and columbic efficiency of the cells made with CNT-microfiber paper were comparable against the devices with metallic and CNT sheet (bucky paper) current collectors.

Paper-like structure of the CNT-microfiber current collector provides more flexibility and better interface adhesion for active materials. It has been shown that the paper can be used with a wide range of active materials having various working voltages and also provides better flexibility. Moreover, the LbL coating process of CNT-microfiber paper have only 10.1 $\mu g/cm^2$ CNT loading and results in resistivity of 1.94 $k\Omega - cm$. Thus, the developed paper-based lithium-ion battery is more cost-effective compared to the non-metallic current collectors. The LCO, LTO, LMO half-cells and the LTO/LCO full-cell were fabricated and tested in this project. The capacities of half-cells were measured 150 mAh/g for LCO, 158 mAh/g for LTO, and 130 mAh/g for LMO. The capacity of the LTO/LCO full-cell was also measured 126 mAh/g at $C/5$ rate. The presented platform is expected to lead in to all solid-state flexible cells with high voltage range and high capacity. Batteries using

CNT-microfiber paper current collectors have a wide-range of applications, in particular in applications where flexibility and lightweight are essentials. Although these batteries are providing comparable capacities with metallic cells, using liquid electrolyte is a challenge to provide a complete flexible lithium-ion battery. In addition, higher resistance of the CNT-microfiber paper is a limitation of these batteries to work with higher currents.

5.2 Future recommendations

Major focus of this research was the use of CNT-microfiber paper as a current collector in lithium ion battery. It has shown that the CNT-microfiber paper can be used with various active materials and can produce more flexibility than metallic current collector. Although all solid-state paper based lithium ion batteries has been identified as one of the principal applications of the developed platform most of the study needed to achieve it has not been conducted and has been identified as the future work of the presented research. Additional details on future work to realize all solid state paper based cell are discussed below:

- As the only non-solid part inside the cell at this time is the electrolyte, fabrication of a high ionic conductive solid electrolyte is the major step in the realization of solid-state lithium ion batteries.
- The research about ionic conductive polymers such as $PVDF$ or PEO with different ionic conductive salts should be conducted.
- The paper based solid separators must also be investigated. More research is needed about the paper based separators in lithium ion cells and include the lithium salts into the paper to make a solid paper based electrolyte.

- The CNT-microfiber paper can be redeveloped and enhanced to provide higher conductivity.
- The mathematical model of the battery can also be provided.

By fabricating a solid electrolyte and enhancing the conductivity of the paper, an all solid-state battery can be fabricated. Increasing the conductivity of the paper can provide denser electron collectors to provide more flexibility. Furthermore, another research is conducted to fabricate a safe and reliable solid electrolyte for flexible lithium-ion batteries. Ionic conductive polymers can be used as the solid electrolyte inside a lithium-ion battery. Because the ionic conductivity of these polymers is not comparable with the liquid electrolytes, a filler material or a lithium salt must be added to the polymer to provide better ionic conductivity. $PVDF$ and polyethylene oxide (PEO) are some of the polymers that were used in fabrication of a solid electrolyte. These polymers can provide the ionic conductivity between 10^{-6} to 10^{-5} S/cm. Furthermore, $LiPF_6$, and $LiTFSi$ with silicon nanoparticles can be used as the ionic conductive materials and fillers to enhance the ionic conductivity of the solid electrolytes. In the next step of this project another research must be conducted to provide a solid state separator for the flexible, all solid state, paper-based battery.

LIST OF REFERENCES

LIST OF REFERENCES

[1] M. A. J. M. Tarascon, "Issues and challenges facing rechargeable lithium batteries," *Nature*, vol. 414, pp. 359–367, 2001.

[2] P. Van den Bossche, F. Vergels, J. Van Mierlo, J. Matheys, and W. Van Autenboer, "Subat: An assessment of sustainable battery technology," *Journal of Power Sources*, vol. 162, no. 2, pp. 913–919, 2006.

[3] T. B. Reddy, *Linden's Handbook of Batteries*, vol. 4. McGraw-Hill, 2011.

[4] L. Lam, "A practical circuit-based model for state of health estimation of li-ion battery cells in electric vehicles," Master's thesis, Online: http://www.eclectic.eu/images/MScthesis_LongLamv3.pdf, 2011 (Accessed May, 2013).

[5] J. Chen, C. Buhrmester, and J. R. Dahn, "Chemical overcharge and overdischarge protection for lithium-ion batteries," *Electrochemical and Solid-State Letters*, vol. 8, no. 1, pp. A59–A62, 2005.

[6] M. Thackeray, "Lithium-ion batteries: An unexpected conductor," *Nature Materials*, vol. 1, pp. 81–82, 2002.

[7] M. Yoshio, R. J. Brodd, and A. Kozawa, *Lithium-ion batteries: science and technologies*. Springer, 2009.

[8] P. Hiralal, S. Imaizumi, H. E. Unalan, H. Matsumoto, M. Minagawa, M. Rouvala, A. Tanioka, and G. A. J. Amaratunga, "Nanomaterial-enhanced all-solid flexible zinccarbon batteries," *ACS Nano*, vol. 4, no. 5, pp. 2730–2734, 2010.

[9] L. Hu, J. W. Choi, Y. Yang, S. Jeong, F. La Mantia, L.-F. Cui, and Y. Cui, "Highly conductive paper for energy-storage devices," *Proceedings of the National Academy of Sciences*, vol. 106, no. 51, pp. 21490–21494, 2009.

[10] B. G. Park, J. H. Ryu, W. Y. Choi, and Y. J. Park, "Fabrication of 3-dimensional limn2o4 thin film," *Bulletin of the Korean Chemical Society*, vol. 30, no. 3, pp. 653–656, 2009.

[11] J. Park, J. H. Seo, G. Plett, W. Lu, and A. M. Sastry, "Numerical simulation of the effect of the dissolution of limn2o4 particles on li-ion battery performance," *Electrochemical and Solid-State Letters*, vol. 14, no. 2, pp. A14–A18, 2011.

[12] T. Tabuchi, N. Hochgatterer, Z. Ogumi, and M. Winter, "Ternary snsbco alloy film as new negative electrode for lithium-ion cells," *Journal of Power Sources*, vol. 188, no. 2, pp. 552–557, 2009.

[13] H. Shin and M. Liu, "Threedimensional porous coppertin alloy electrodes for rechargeable lithium batteries," *Advanced Functional Materials*, vol. 15, no. 4, pp. 582–586, 2005.

[14] M. Agarwal, Q. Xing, B. S. Shim, N. Kotov, K. Varahramyan, and Y. Lvov, "Conductive paper from lignocellulose wood microfibers coated with a nanocomposite of carbon nanotubes and conductive polymers," *Nanotechnology*, vol. 20, no. 21, p. 215602, 2009.

[15] S. Y. An, I. C. Jeong, M.-S. Won, E. D. Jeong, and Y.-B. Shim, "Effect of additives in peo/paa/pmaa composite solid polymer electrolytes on the ionic conductivity and li ion battery performance," *Journal of applied electrochemistry*, vol. 39, no. 9, pp. 1573–1578, 2009.

[16] G. Nystrom, A. Razaq, M. Strmme, L. Nyholm, and A. Mihranyan, "Ultrafast all-polymer paper-based batteries," *Nano letters*, vol. 9, no. 10, pp. 3635–3639, 2009.

[17] G. B. Appetecchi, P. Romagnoli, and B. Scrosati, "Composite gel membranes: a new class of improved polymer electrolytes for lithium batteries," *Electrochemistry Communications*, vol. 3, no. 6, pp. 281–284, 2001.

[18] J. B. Bates, N. J. Dudney, B. Neudecker, A. Ueda, and C. D. Evans, "Thin-film lithium and lithium-ion batteries," *Solid State Ionics*, vol. 135, no. 14, pp. 33–45, 2000.

[19] J. O. Besenhard, "Handbook of battery materials," *Handbook of Battery Materials, by JO Besenhard (Editor), pp. 648. ISBN 3-527-29469-4. Wiley-VCH, April 1999.*, vol. 1, 1999.

[20] Y. Hamon, A. Douard, F. Sabary, C. Marcel, P. Vinatier, B. Pecquenard, and A. Levasseur, "Influence of sputtering conditions on ionic conductivity of lipon thin films," *Solid State Ionics*, vol. 177, no. 34, pp. 257–261, 2006.

[21] A. Hayashi, T. Ohtomo, F. Mizuno, K. Tadanaga, and M. Tatsumisago, "All-solid-state li/s batteries with highly conductive glassceramic electrolytes," *Electrochemistry Communications*, vol. 5, no. 8, pp. 701–705, 2003.

[22] A. Herold, "Recherches sur les composes d'insertion du graphite," *Bull. Soc. Chim. Fr*, vol. 187, no. 7-8, pp. 999–1012, 1955.

[23] A. K. Padhi, K. S. Nanjundaswamy, and J. B. Goodenough, "Phosphoolivines as positiveelectrode materials for rechargeable lithium batteries," *Journal of The Electrochemical Society*, vol. 144, no. 4, pp. 1188–1194, 1997.

[24] M. Thackeray, W. David, P. Bruce, and J. Goodenough, "Lithium insertion into manganese spinels," *Materials Research Bulletin*, vol. 18, no. 4, pp. 461–472, 1983.

[25] N. Aliahmad, M. Agarwal, S. Shrestha, and K. Varahramyan, "Paper-based lithium-ion batteries using carbon nanotube-coated wood microfibers," *Nanotechnology, IEEE Transactions on*, vol. 12, no. 3, pp. 408–412, 2013.

[26] X. Yu, J. Bates, G. Jellison, and F. Hart, "A stable thinfilm lithium electrolyte: Lithium phosphorus oxynitride," *Journal of the electrochemical society*, vol. 144, no. 2, pp. 524–532, 1997.

[27] D. Heider, D. Oesten, P. Scrosati, and F. Croce, "Polymer electrolyte membrane for use in lithium batteries." EP Patent 1,096,591, 2001.

[28] D. M. DeLongchamp and P. T. Hammond, "Highly ion conductive poly(ethylene oxide)-based solid polymer electrolytes from hydrogen bonding layer-by-layer assembly," *Langmuir*, vol. 20, no. 13, pp. 5403–5411, 2004.

[29] J. Seo, J. L. Lutkenhaus, J. Kim, P. T. Hammond, and K. Char, "Effect of the layer-by-layer (lbl) deposition method on the surface morphology and wetting behavior of hydrophobically modified peo and paa lbl films," *Langmuir*, vol. 24, no. 15, pp. 7995–8000, 2008.

[30] J. Choi, D. J. Lee, Y. M. Lee, Y. Lee, K. M. Kim, J. Park, and K. Y. Cho, "Silicon nanofibrils on a flexible current collector for bendable lithiumion battery anodes," *Advanced Functional Materials*, vol. 23, pp. 2108–2114, 2012.

[31] L. Hu, H. Wu, F. La Mantia, Y. Yang, and Y. Cui, "Thin, flexible secondary li-ion paper batteries," *ACS nano*, vol. 4, no. 10, pp. 5843–5848, 2010.

[32] J. Boyea, R. Camacho, S. Sturano, and W. Ready, "Carbon nanotube-based supercapacitors: technologies and markets," *Nanotechnology Law and Business*, vol. 4, p. 19, 2007.

[33] D. N. Futaba, K. Hata, T. Yamada, T. Hiraoka, Y. Hayamizu, Y. Kakudate, O. Tanaike, H. Hatori, M. Yumura, and S. Iijima, "Shape-engineerable and highly densely packed single-walled carbon nanotubes and their application as supercapacitor electrodes," *Nature Materials*, vol. 5, no. 12, pp. 987–994, 2006.

[34] C. Emmenegger, P. Mauron, P. Sudan, P. Wenger, V. Hermann, R. Gallay, and A. Zttel, "Investigation of electrochemical double-layer (ecdl) capacitors electrodes based on carbon nanotubes and activated carbon materials," *Journal of Power Sources*, vol. 124, no. 1, pp. 321–329, 2003.

[35] D. S. Lashmore, E. Silverman, E. Towle, C. Brennan, M. White, B. White, M. Schauer, and C. Timoney, "Synthesis and properties of cnt composites," vol. 2, pp. 212–213, 2010.

[36] K. J. Loh, J. Kim, J. P. Lynch, N. W. S. Kam, and N. A. Kotov, "Multifunctional layer-by-layer carbon nanotubepolyelectrolyte thin films for strain and corrosion sensing," *Smart Materials and Structures*, vol. 16, no. 2, p. 429, 2007.

[37] J. Yang, S.-C. Wang, X.-Y. Zhou, and J. Xie, "Electrochemical behaviors of functionalized carbon nanotubes in LiPF6/EC+ DMC electrolyte," *International Journal of Electrochemical Science*, vol. 7, pp. 6118–6126, 2012.

[38] D. Steingart, C. C. Ho, J. Salminen, J. W. Evans, and P. K. Wright, "Dispenser printing of solid polymer-ionic liquid electrolytes for lithium ion cells," in *Polymers and Adhesives in Microelectronics and Photonics, 2007. Polytronic 2007. 6th International Conference on*, pp. 261–264, IEEE.

[39] M. Agarwal, Y. Lvov, and K. Varahramyan, "Conductive wood microfibres for smart paper through layer-by-layer nanocoating," *Nanotechnology*, vol. 17, no. 21, p. 5319, 2006.

[40] J. Tarascon and M. Armand, "Building better batteries," *Nature*, vol. 451, no. 1, pp. 652–657, 2008.

[41] J. W. Fergus, "Recent developments in cathode materials for lithium ion batteries," *Journal of Power Sources*, vol. 195, no. 4, pp. 939–954, 2010.

[42] W. Fang, O. J. Kwon, and C. Wang, "Electrochemicalthermal modeling of automotive li ion batteries and experimental validation using a threeelectrode cell," *International Journal of Energy Research*, vol. 34, no. 2, pp. 107–115, 2010.

[43] B. Zimmermann, *Integration of carbon nanotubes in lithium-ion traction batteries from an environmental perspective*. PhD thesis, Online: http://www.fb06.fh-muenchen.de/fb/images/img_upld/arbeiten/01551.pdf, 2012 (Accessed July, 2013).

[44] C. Mikolajczak, M. Kahn, K. White, and R. T. Long, *Lithium-Ion Batteries Hazard and Use Assessment*. Springer, 2012.

[45] P. Arora, R. E. White, and M. Doyle, "Capacity fade mechanisms and side reactions in lithiumion batteries," *Journal of the Electrochemical Society*, vol. 145, no. 10, pp. 3647–3667, 1998.

[46] N. D. Williard, *Degradation Analysis and Health Monitering of Lithium Ion Batteries*. PhD thesis, University of Maryland, http://drum.lib.umd.edu/handle/1903/12381, 2011 (Accessed July, 2013).

[47] R. Spotnitz, "Simulation of capacity fade in lithium-ion batteries," *Journal of Power Sources*, vol. 113, no. 1, pp. 72–80, 2003.

[48] M. Gateshki, S.-J. Hwang, D. H. Park, Y. Ren, and V. Petkov, "Structure of nanocrystalline alkali metal manganese oxides by the atomic pair distribution function technique," *The Journal of Physical Chemistry B*, vol. 108, no. 39, pp. 14956–14963, 2004.

[49] J. S. Do and C. H. Weng, "Electrochemical and charge/discharge properties of the synthesized cobalt oxide as anode material in li-ion batteries," *Journal of Power Sources*, vol. 159, no. 1, pp. 323–327, 2006.

[50] T. Takeuchi, T. Kyuna, H. Morimoto, and S. i. Tobishima, "Influence of surface modification of licoo 2 by organic compounds on electrochemical and thermal properties of li/licoo2 rechargeable cells," *Journal of Power Sources*, vol. 196, no. 5, pp. 2790–2801, 2011.

[51] S. H. Kim, K. H. Lee, B. S. Seong, G. H. Kim, J. S. Kim, and Y. S. Yoon, "Synthesis and structural properties of lithium titanium oxide powder," *Korean Journal of Chemical Engineering*, vol. 23, no. 6, pp. 961–964, 2006.

[52] D. Peramunage and K. Abraham, "Preparation of micronsized li4ti5 o 12 and its electrochemistry in polyacrylonitrile electrolytebased lithium cells," *Journal of the Electrochemical Society*, vol. 145, no. 8, pp. 2609–2615, 1998.

[53] K. Zaghib, M. Simoneau, M. Armand, and M. Gauthier, "Electrochemical study of li4ti5o12 as negative electrode for li-ion polymer rechargeable batteries," *Journal of Power Sources*, vol. 8182, no. 0, pp. 300–305, 1999.

[54] E. M. Sorensen, S. J. Barry, H. K. Jung, J. M. Rondinelli, J. T. Vaughey, and K. R. Poeppelmeier, "Three-dimensionally ordered macroporous li4ti5o12: effect of wall structure on electrochemical properties," *Chemistry of Materials*, vol. 18, no. 2, pp. 482–489, 2005.

[55] S. Zhang, K. Xu, and T. Jow, "A thermal stabilizer for lipf6-based electrolytes of li-ion cells," *Electrochemical and Solid-State Letters*, vol. 5, no. 9, pp. A206–A208, 2002.

[56] X. L. Wang, W. N. Wang, and D. X. Wang, "Experimental investigation on separation performance of nanofiltration membranes for inorganic electrolyte solutions," *Desalination*, vol. 145, no. 13, pp. 115–122, 2002.

[57] J. Y. Song, Y. Y. Wang, and C. C. Wan, "Review of gel-type polymer electrolytes for lithium-ion batteries," *Journal of Power Sources*, vol. 77, no. 2, pp. 183–197, 1999.

[58] R. Kanno and M. Murayama, "Lithium ionic conductor thio-lisicon: The Li2S GeS2 P2S5 system," *Journal of The Electrochemical Society*, vol. 148, no. 7, pp. A742–A746, 2001.

[59] A. H. Whitehead and M. Schreiber, "Current collectors for positive electrodes of lithium-based batteries," *Journal of The Electrochemical Society*, vol. 152, no. 11, pp. A2105–A2113, 2005.

[60] G. X. Wang, L. Yang, Y. Chen, J. Z. Wang, S. Bewlay, and H. K. Liu, "An investigation of polypyrrole-lifepo4 composite cathode materials for lithium-ion batteries," *Electrochimica Acta*, vol. 50, no. 24, pp. 4649–4654, 2005.

[61] M. S. Yazici, D. Krassowski, and J. Prakash, "Flexible graphite as battery anode and current collector," *Journal of Power Sources*, vol. 141, no. 1, pp. 171–176, 2005.

[62] S. C. Nagpure, R. Gregory Downing, B. Bhushan, and S. Babu, "Discovery of lithium in copper current collectors used in batteries," *Scripta Materialia*, vol. 67, no. 7-8, pp. 669–672, 2012.

[63] H. Gwon, H. S. Kim, K. U. Lee, D. H. Seo, Y. C. Park, Y. S. Lee, B. T. Ahn, and K. Kang, "Flexible energy storage devices based on graphene paper," *Energy Environmental Science*, vol. 4, no. 4, pp. 1277–1283, 2011.

[64] G. Zhou, D.-W. Wang, F. Li, L. Zhang, N. Li, Z.-S. Wu, L. Wen, G. Q. Lu, and H.-M. Cheng, "Graphene-wrapped fe3o4 anode material with improved reversible capacity and cyclic stability for lithium ion batteries," *Chemistry of Materials*, vol. 22, no. 18, pp. 5306–5313, 2010.

[65] H. Park, A. K. Lim, A. P. Alivisatos, J. Park, and P. L. McEuen, "Fabrication of metallic electrodes with nanometer separation by electromigration," *Applied Physics Letters*, vol. 75, no. 2, pp. 301–303, 1999.

[66] K. Peng, J. Jie, W. Zhang, and S. T. Lee, "Silicon nanowires for rechargeable lithium-ion battery anodes," *Applied Physics Letters*, vol. 93, no. 3, pp. 033105–033105–3, 2008.

[67] J. Graetz, C. Ahn, R. Yazami, and B. Fultz, "Highly reversible lithium storage in nanostructured silicon," *Electrochemical and Solid-State Letters*, vol. 6, no. 9, pp. A194–A197, 2003.

[68] S. W. Lee, B. M. Gallant, H. R. Byon, P. T. Hammond, and Y. Shao-Horn, "Nanostructured carbon-based electrodes: bridging the gap between thin-film lithium-ion batteries and electrochemical capacitors," *Energy Environmental Science*, vol. 4, no. 6, pp. 1972–1985, 2011.

[69] B. Liu, J. Zhang, X. Wang, G. Chen, D. Chen, C. Zhou, and G. Shen, "Hierarchical three-dimensional znco2o4 nanowire arrays/carbon cloth anodes for a novel class of high-performance flexible lithium-ion batteries," *Nano Letters*, vol. 12, no. 6, pp. 3005–3011, 2012.

[70] K. H. Seng, J. Liu, Z. P. Guo, Z. X. Chen, D. Jia, and H. K. Liu, "Free-standing v2o5 electrode for flexible lithium ion batteries," *Electrochemistry Communications*, vol. 13, no. 5, pp. 383–386, 2011.

[71] Y. Li, B. Tan, and Y. Wu, "Mesoporous co3o4 nanowire arrays for lithium ion batteries with high capacity and rate capability," *Nano Letters*, vol. 8, no. 1, pp. 265–270, 2007.

[72] A. W. Martinez, S. T. Phillips, G. M. Whitesides, and E. Carrilho, "Diagnostics for the developing world: microfluidic paper-based analytical devices," *Analytical chemistry*, vol. 82, no. 1, pp. 3–10, 2009.

[73] L. Zhang, X. Sun, Z. Hu, C. Yuan, and C. Chen, "Rice paper as a separator membrane in lithium-ion batteries," *Journal of Power Sources*, vol. 204, pp. 149–154, 2012.

[74] S.-J. Chun, E. S. Choi, E. H. Lee, J. H. Kim, S. Y. Lee, and S. Y. Lee, "Eco-friendly cellulose nanofiber paper-derived separator membranes featuring tunable nanoporous network channels for lithium-ion batteries," *Journal of Materials Chemistry*, vol. 22, no. 32, pp. 16618–16626, 2012.

[75] G. Nystrom, A. Mihranyan, A. Razaq, T. Lindstrom, L. Nyholm, and M. Strmme, "A nanocellulose polypyrrole composite based on microfibrillated cellulose from wood," *The Journal of Physical Chemistry B*, vol. 114, no. 12, pp. 4178–4182, 2010.

[76] M.-C. Liu, L.-B. Kong, P. Zhang, Y.-C. Luo, and L. Kang, "Porous wood carbon monolith for high-performance supercapacitors," *Electrochimica Acta*, vol. 60, pp. 443–448, 2012.

[77] S. F. Lux, M. Schmuck, G. B. Appetecchi, S. Passerini, M. Winter, and A. Balducci, "Lithium insertion in graphite from ternary ionic liquidlithium salt electrolytes: Ii. evaluation of specific capacity and cycling efficiency and stability at room temperature," *Journal of Power Sources*, vol. 192, no. 2, pp. 606–611, 2009.

[78] T. Piao, S. Park, C. Doh, and S. Moon, "Intercalation of lithium ions into graphite electrodes studied by ac impedance measurements," *Journal of The Electrochemical Society*, vol. 146, no. 8, pp. 2794–2798, 1999.

[79] A. D. Pasquier, I. Plitz, J. Gural, F. Badway, and G. Amatucci, "Power-ion battery: bridging the gap between li-ion and supercapacitor chemistries," *Journal of Power Sources*, vol. 136, no. 1, pp. 160–170, 2004.